

ผลของการออกแบบอุปกรณ์ภายในห้องที่ใช้อากาศช่วยในการไหลวนที่มีต่อพฤติกรรมทางด้านไฮโดรไดนามิกส์
และอัตราการถ่ายเทมวลสารระหว่างอากาศและน้ำ



นางสาวฉัตรณี วรพงศธร

สถาบันวิทยบริการ

จุฬาลงกรณ์มหาวิทยาลัย

วิทยานิพนธ์นี้เป็นส่วนหนึ่งของการศึกษาตามหลักสูตรปริญญาวิศวกรรมศาสตรมหาบัณฑิต

สาขาวิชาวิศวกรรมเคมี ภาควิชาวิศวกรรมเคมี


คณะวิศวกรรมศาสตร์ จุฬาลงกรณ์มหาวิทยาลัย

ปีการศึกษา 2543

ISBN 974-346-111-6

ลิขสิทธิ์ของจุฬาลงกรณ์มหาวิทยาลัย

EFFECT OF DESIGN CONFIGURATIONS ON HYDRODYNAMIC BEHAVIOR AND GAS-LIQUID
MASS TRANSFER IN THE INTERNAL-LOOP AIRLIFT CONTACTOR



Miss Thanathorn Vorapongsathorn

สถาบันวิทยบริการ
จุฬาลงกรณ์มหาวิทยาลัย

A Thesis Submitted in Partial Fulfillment of the Requirements
for the Degree of Master of Engineering in Chemical Engineering
Department of Chemical Engineering

Faculty of Engineering
Chulalongkorn University
Academic Year 2000
ISBN 974-346-111-6

Thesis Title Effect of design configurations on hydrodynamic behavior and
 gas-liquid mass transfer in the internal-loop airlift contactor
By Miss Thanathorn Vorapongsathorn
Department Chemical Engineering
Thesis Advisor Prasert Pavasant, Ph.D.

Accepted by the Faculty of Engineering, Chulalongkorn University in Partial
Fulfillment of the Requirements for the Master's Degree

.....Dean of Faculty of Engineering
(Professor Somsak Panyakeow, D.Eng)

THESIS COMMITTEE

.....Chairman
(Professor Piyasarn Praserttham, Dr.Eng.)

.....Thesis Advisor
(Prasert Pavasant, Ph.D.)

.....Member
(Associate Professor Tawatchai Charinpanitkul, Ph.D.)

.....Member
(Varun Taepaisitphongse, Ph.D.)

สถาบันทศยบริการ
จุฬาลงกรณ์มหาวิทยาลัย

ธนธรณ์ วรพงศธร: ผลของการออกแบบอุปกรณ์ภายในท่อที่ใช้อากาศช่วยในการไหลวนที่มีต่อพฤติกรรมทางด้านไฮโดรไดนามิกส์และอัตราการถ่ายเทมวลสารระหว่างอากาศและน้ำ (EFFECT OF DESIGN CONFIGURATIONS ON HYDRODYNAMIC BEHAVIOR AND GAS-LIQUID MASS TRANSFER IN THE INTERNAL-LOOP AIRLIFT CONTACTOR) อ. ที่ปรึกษา: อาจารย์ ดร. ประเสริฐ ภาวสันต์, 77 หน้า. ISBN 974-346-111-6.

งานวิจัยนี้ศึกษาเกี่ยวกับผลของการออกแบบอุปกรณ์ภายใน “ท่อที่ใช้อากาศช่วยในการไหลวน” ที่มีต่อพฤติกรรมทางด้านอุทกพลศาสตร์และอัตราการถ่ายเทมวลสารระหว่างอากาศและน้ำ การออกแบบอุปกรณ์ท่อภายใน (Draft tube) ที่ศึกษาแบ่งได้เป็น 3 ลักษณะคือ (1) ท่อภายในที่มีลักษณะเป็นทรงกระบอก (2) ท่อภายในที่มีลักษณะเป็นทรงกระบอกและมีแผ่นกั้นติดตั้งอยู่ภายใน (3) ท่อภายในที่มีลักษณะเป็นทรงกระบอกที่แบ่งออกเป็นสองส่วนในแนวตั้ง คือ ส่วนบนและส่วนล่าง ค่ากำลังงานจำเพาะที่ใช้ในแต่ละการทดลองอยู่ในช่วง 55 ถึง 357 วัตต์ต่อลูกบาศก์เมตร ซึ่งจากการศึกษาพบว่าแผ่นกั้นที่ใส่เข้าไปในท่อภายในนั้นจะขัดขวางการไหลของของเหลวและฟองอากาศ นอกจากนี้การใส่แผ่นกั้นจะทำให้ฟองอากาศมีการรวมตัวกันมากขึ้นส่งผลให้ขนาดของฟองอากาศใหญ่ขึ้นและพื้นที่ผิวสัมผัสระหว่างก๊าซกับของเหลวจะลดลงตามลำดับ อย่างไรก็ตามแผ่นกั้นที่ใส่นั้นจะทำให้ระบบเกิดความปั่นป่วนสูงซึ่งจะเป็นการเพิ่มค่าสัมประสิทธิ์การถ่ายเทมวลสารและเนื่องจากการเพิ่มขึ้นของค่าสัมประสิทธิ์การถ่ายเทมวลสารมีอิทธิพลมากกว่าการลดลงของพื้นที่ผิวสัมผัสระหว่างก๊าซกับของเหลว ดังนั้นค่าสัมประสิทธิ์การถ่ายเทมวลสารรวมระหว่างก๊าซและของเหลวในท่อที่ใส่แผ่นกั้นจึงมีค่ามากกว่าในท่อภายในแบบทรงกระบอกธรรมดา แต่ที่ค่ากำลังงานจำเพาะสูงกว่า 200 วัตต์ต่อลูกบาศก์เมตรพบว่าอิทธิพลของแผ่นกั้นที่มีต่อค่าสัมประสิทธิ์การถ่ายเทมวลสารรวมลดลงเนื่องจากการเกิดพื้นที่ที่ไม่มีถ่ายเทมวลสารบริเวณใต้แผ่นกั้นเหล่านี้ ในการศึกษาในระบบที่มีการใส่ท่อภายในแบบแยกบนและล่างพบว่าจะมีชั้นความต้านทานเกิดขึ้นบริเวณส่วนต่อระหว่างท่อชั้นบนและชั้นล่างซึ่งชั้นความต้านทานนี้จะขัดขวางการไหลของของเหลวส่งผลให้ค่าความเร็วของของเหลวในระบบที่มีการใส่ท่อภายในแบบแยกบนและล่างต่ำกว่าในระบบที่มีการใส่ท่อภายในแบบทรงกระบอกธรรมดา อย่างไรก็ตามพบว่าท่อภายในแบบแยกบนและล่างจะทำให้ฟองอากาศที่มีขนาดเล็กมีจำนวนเพิ่มมากขึ้นเมื่อเทียบกับระบบที่ทำในท่อภายในแบบทรงกระบอกธรรมดา ซึ่งการเพิ่มจำนวนของฟองอากาศขนาดเล็กจะทำให้ค่าพื้นที่ผิวสัมผัสระหว่างของเหลวและก๊าซเพิ่มขึ้นด้วย ดังนั้นค่าสัมประสิทธิ์การถ่ายเทมวลสารรวมในระบบที่ใส่ท่อภายในแบบแยกบนและล่างจึงมีค่ามากกว่าในระบบปกติ แต่ที่ค่ากำลังงานจำเพาะสูงกว่า 155 วัตต์ต่อลูกบาศก์เมตรพบว่าอัตราการเพิ่มของค่าสัมประสิทธิ์การถ่ายเทมวลสารรวมลดลงอย่างมาก

ภาควิชา วิศวกรรมเคมี
สาขาวิชา วิศวกรรมเคมี
ปีการศึกษา 2543

ลายมือชื่อนิสิต
ลายมือชื่ออาจารย์ที่ปรึกษา
ลายมือชื่ออาจารย์ที่ปรึกษาร่วม -

417 0325721 : MAJOR CHEMICAL ENGINEERING

KEY WORD: AIRLIFT CONTACTOR / HYDRODYNAMIC BEHAVIOR / MASS TRANSFER / DRAFT TUBE DESIGN / DESIGN CONFIGURATION

THANATHORN VORAPONGSATHORN: EFFECT OF DESIGN CONFIGURATIONS ON HYDRODYNAMIC BEHAVIOR AND GAS-LIQUID MASS TRANSFER IN THE INTERNAL-LOOP AIRLIFT CONTACTOR. THESIS ADVISOR: PRASERT PAVASANT, Ph.D. 77 pp. ISBN 974-346-111-6.

The effect of design configurations on hydrodynamic behavior and gas-liquid mass transfer in three types of internal-loop airlift contactors were investigated. The model systems were (i) conventional concentric tube airlift contactor so-called ALC, (ii) ALC with baffles installed in the riser so called ALC-B, and (iii) ALC with a vertically split draft tube so called ALC-S. Each experiment was performed with a specific power input (P_G/V_L) ranging from 55-357 W/m³. Baffles were found to obstruct a flow of liquid and gas bubbles, and to induce more bubble coalescence resulting in a larger bubble diameter. This negatively influenced gas-liquid interfacial area (a) in the contactor. However, the baffles encouraged more turbulence in the system and led to a higher value of mass transfer coefficient (k_L). The effect on " k_L " was found to be more outstanding than the effect on " a " and thus the overall gas-liquid mass transfer coefficient ($k_L a$) in the ALC-B was higher than in the ALC. This is true only for the system at the specific power input less than 200 W/m³. At higher values of P_G/V_L the effect of baffles disappeared and the performance of ALC-B was close to that of the conventional ALC due to the existence of dead zones below each baffle plate. In the ALC-S it was expected that there was a resistant layer in the space between the upper and lower draft tubes of the contactor which obstructed the liquid flow. This resulted in a lower liquid circulation in the ALC-S when compared to the liquid circulation in the ALC. However, it was observed that this configuration facilitated the occurrence of small bubbles resulting in an increase in the specific gas-liquid interfacial area (a). Due to this larger " a ", a more favorable value of mass transfer was obtained in the ALC-S than in the ALC. However, at high P_G/V_L (> 200 W/m³) the effect of vertically split draft tube on the mass transfer tended to significantly decrease. The reason for this phenomenon can not be realized from the existing experimental setup, and more investigation is needed.

ภาควิชา วิศวกรรมเคมี
สาขาวิชา วิศวกรรมเคมี
ปีการศึกษา 2543

ลายมือชื่อนิติ
ลายมือชื่ออาจารย์ที่ปรึกษา
ลายมือชื่ออาจารย์ที่ปรึกษาร่วม -

ACKNOWLEDGEMENTS

I would like to express my sincere gratitude to Dr. Prasert Pavasant, my advisor, for his invaluable guidance and suggestions, positive criticism, and generous supervision throughout the master program. I am grateful to Professor Dr. Piyasan Praserttham, Chairman of the committee, Associate Professor Dr. Tawatchai Charinpanitkul and Dr. Varun Taepaisitphongse, members of thesis committees, for many valuable comments.

My work could not have been carried out without the help of my best friend, Miss Pornthip Wongsuchoto. I would like to express my gratitude to her. Of course, I wish to express my appreciation to my lovely friends, Miss Purida Pimarnmard, Miss Narumon Chareontra, Miss Vichaya Vichapai Bunnark, and Miss Thida Thadsanarapan for their encouragements during my study. Moreover, special thanks to all members of the Environmental and the Biochemical Engineering groups for their nice relationship.

Finally, I would like to express my highest gratitude to my parents for their inspiration and invaluable support all the time.

สถาบันวิทยบริการ
จุฬาลงกรณ์มหาวิทยาลัย

CONTENTS

| | PAGE |
|--|------|
| ABSTRACT (IN THAI)..... | iv |
| ABSTRACT (IN ENGLISH)..... | v |
| ACKNOWLEDGEMENTS..... | vi |
| LIST OF TABLES..... | ix |
| LIST OF FIGURES..... | x |
| NOMENCLATURE..... | xii |
| CHAPTER | |
| 1 INTRODUCTION..... | 1 |
| 1.1 General Ideas..... | 1 |
| 1.2 Objectives..... | 2 |
| 1.3 Scopes of Work..... | 3 |
| 2 BACKGROUNDS..... | 4 |
| 2.1 Airlift Contactor: Anatomy..... | 4 |
| 2.2 Background: Hydrodynamic Behavior of ALCs..... | 6 |
| 2.3 Background: Mass Transfer of ALCs..... | 11 |
| 3 EXPERIMENT..... | 14 |
| 3.1 Experimental Equipment..... | 14 |
| 3.2 Experimental Procedure..... | 17 |
| 3.3 Methods of Measurement..... | 19 |
| 4 RESULTS AND DISCUSSION..... | 23 |
| 4.1 Effect of Specific Power Input on Hydrodynamic Behavior and Mass Transfer Performance in ALCs..... | 23 |
| 4.2 Effect of Baffles on Hydrodynamic Behavior and Mass Transfer Performance in ALCs..... | 28 |
| 4.3 Effect of Vertically Split Draft Tube on Hydrodynamic Behavior and Mass Transfer Performance in ALCs..... | 33 |
| 5 CONCLUSIONS AND RECOMMENDATIONS..... | 55 |
| 5.1 Effect of Specific Power Input on Hydrodynamic | |

| | |
|--|----|
| Behavior and Mass Transfer Performance in ALCs..... | 55 |
| 5.2 Effect of Baffles on Hydrodynamic Behavior and Mass Transfer Performance in ALCs..... | 57 |
| 5.3 Effect of Vertically Split Draft Tube on Hydrodynamic Behavior and Mass Transfer Performance in ALCs..... | 59 |
| 5.4 Concluding Remarks..... | 61 |
| REFERENCES..... | 62 |
| APPENDIX: Determination of Various Parameters..... | 67 |
| VITA..... | 77 |



สถาบันวิทยบริการ
จุฬาลงกรณ์มหาวิทยาลัย

LIST OF TABLES

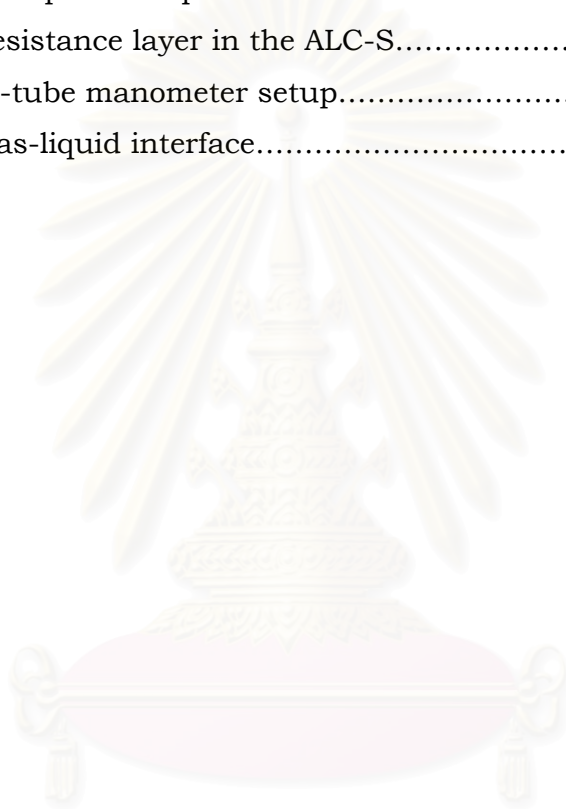
| TABLE | PAGE |
|--|------|
| 3.1 Dimension of the employed airlift contactors..... | 16 |
| 4.1 Expressions showing the relationships between slip velocity and other parameters..... | 25 |
| 5.1 Expressions showing the relationships between hydrodynamic and mass transfer parameters with P_G/V_L in the ALC..... | 56 |
| 5.2 Expressions showing the relationships between hydrodynamic and mass transfer parameters with P_G/V_L in the ALC-B..... | 58 |
| 5.3 Expressions showing the relationships between hydrodynamic and mass transfer parameters with P_G/V_L in the ALC-S..... | 60 |

สถาบันวิทยบริการ
จุฬาลงกรณ์มหาวิทยาลัย

LIST OF FIGURES

| FIGURE | PAGE |
|--|------|
| 2.1 Types of airlift contactors..... | 4 |
| 2.2 Basic structure of the airlift contactor..... | 6 |
| 3.1 Experimental setup of the airlift contactor..... | 15 |
| 3.2 The configuration of the airlift contactors employed in this work..... | 16 |
| 3.3 Dimensions of airlift contactors employed in this work..... | 17 |
| 4.1 Relationship between liquid velocity and specific power input in the ALC | 36 |
| 4.2 Relationship between gas holdups and specific power input in the ALCs..... | 37 |
| 4.3 Relationship between slip velocities and specific power input in the ALC | 38 |
| 4.4 The mechanism controlling riser gas holdup..... | 39 |
| 4.5 Relationship between mass transfer coefficient and specific power input in the ALC..... | 40 |
| 4.6 Relationship between k_L/d_B and specific power input in various configurations of ALCs..... | 41 |
| 4.7 Relationship between liquid velocity and specific power input in various configurations of ALCs..... | 42 |
| 4.8 Relationship between riser gas holdup and specific power input in various configurations of ALCs..... | 43 |
| 4.9 Relationship between downcomer gas holdup and specific power input in various configurations of ALCs..... | 44 |
| 4.10 Relationship between bubble diameter and specific power input in various configurations of ALCs..... | 45 |
| 4.11 Relationship between overall gas holdup and specific power input in various configurations of ALCs..... | 46 |
| 4.12 Relationship between mass transfer coefficient and specific power input in various configurations of ALCs..... | 47 |
| 4.13 Relationship between slip velocity and riser gas | |

| | |
|---|----|
| holdup in various configurations of ALCs..... | 48 |
| 4.14 Dead zones in the ALC-B..... | 49 |
| 4.15 Relationship between liquid velocity and specific power input in various configurations of ALCs..... | 50 |
| 4.16 Relationship between liquid flowrate and specific power input at the upper and lower parts of ALCs..... | 51 |
| 4.17 The flow path of liquid in the ALC-S..... | 52 |
| 4.18 The resistance layer in the ALC-S..... | 53 |
| A.1 The u-tube manometer setup..... | 69 |
| A.2 The gas-liquid interface..... | 71 |



สถาบันวิทยบริการ
จุฬาลงกรณ์มหาวิทยาลัย

NOMENCLATURE

| | |
|------------|--|
| a_L | specific gas-liquid interfacial area (1/m) |
| A_d | downcomer cross-sectional area (m ²) |
| A_L | total gas-liquid interfacial area (m ²) |
| A_r | riser cross-sectional area (m ²) |
| C | bulk concentration of dissolved oxygen (kg/m ³) |
| ΔC | concentration gradient (kg/m ³) |
| C_0 | initial concentration of dissolved oxygen (kg/m ³) |
| C^* | saturated concentration of dissolved oxygen (kg/m ³) |
| C_G | oxygen concentration in gas-phase (kg/m ³) |
| C_{Gi} | interfacial oxygen concentration on the gas-side (kg/m ³) |
| C_L | instantaneous concentration of oxygen in liquid (kg/m ³) |
| C_{Li} | interfacial concentration on liquid-side (kg/m ³) |
| d_B | bubble diameter (m) |
| D | column diameter (m) |
| D | the molecular diffusivity of oxygen in the film (m ² /s) |
| D_{DT} | draft tube diameter (m) |
| g | gravitational acceleration (m/s ²) |
| Δh | distance between pressure measurement points (m) |
| H_D | liquid dispersion height (m) |
| H_{DT} | draft tube height (m) |
| H_L | unaerated liquid height (m) |
| J_{O_2} | flux of oxygen (kg/m ² .s) |
| k_L | mass transfer coefficient (m/s) |
| $k_L a$ | mass transfer coefficient (1/s) |
| K_L | overall mass transfer coefficient based on liquid film (m/s) |
| L | axial distance (m) |
| L | bottom clearance (m) |
| L_d | distance between measurement points in downcomer (m) |
| L/D_{DT} | ratio between bottom clearance and draft tube diameter (dimensionless) |
| n | number of moles |
| N | number of data or bubbles (dimensionless) |

| | |
|----------------|---|
| P | pressure (kg/m.s ²) |
| ΔP | measured hydrostatic pressure difference (kg/m.s ²) |
| P_{atm} | atmospheric pressure (kg/m.s ²) |
| P_b | pressure at the bottom (kg/m.s ²) |
| P_h | reactor head-space pressure (kg/m.s ²) |
| P_t | pressure at the top (kg/m.s ²) |
| P_G | pneumatic power input (W) |
| P_G/V_L | specific power input (W/m ³) |
| Q_G | gas flow rate (m ³ /s) |
| Q_{G1} | gas flow rate into the ALC-S (m ³ /s) |
| Q_{G2} | gas flow rate into the ALC (m ³ /s) |
| Q_m | molar gas flow rate (kmol/s) |
| R | gas constant (=8314 JK ⁻¹ kmol ⁻¹) |
| t | time (s) |
| t_d | average time in downcomer (s) |
| t_r | average time in riser (s) |
| T | absolute temperature (K) |
| u_{bx} | terminal bubble rise velocity (m/s) |
| \dot{U}_{sg} | local volume of U_{sg} (m/s) |
| U_{sg} | superficial gas velocity (m/s) |
| U_{sgr} | superficial gas velocity in riser (m/s) |
| u_L | liquid velocity (m/s) |
| u_{Ld} | liquid velocity in downcomer (m/s) |
| u_{Llw} | liquid velocity at the lower part of ALC-S (m/s) |
| u_{Lup} | liquid velocity at the upper part of ALC-S (m/s) |
| u_s | slip velocity (m/s) |
| u_G | absolute gas velocity (m/s) |
| \bar{V} | local volume flow (m ³ /s) |
| V_b | initial volume of gas (bottom) (m ³) |
| V_D | dispersion volume (m ³) |
| V_{Dr} | dispersion volume in riser (m ³) |
| V_{Dd} | dispersion volume in downcomer (m ³) |
| V_{Dgs} | dispersion volume in gas-liquid separator (m ³) |

| | |
|---------------------|--|
| V_G | gas volume (m ³) |
| V_L | liquid volume (m ³) |
| V_t | final volume of gas (top) (m ³) |
| $\Delta V/\Delta t$ | volume of gas entering the system within the time interval (m ³ /s) |
| \dot{w} | work done by during isothermal expansion (J) |
| Δz | the difference of liquid height in a manometer (m) |
| Δx | film thickness (m) |

Greek letters

| | |
|---------------------|---|
| ε_d | downcomer gas holdup (dimensionless) |
| ε_{dlw} | downcomer gas holdup at the lower part of ALC-S (dimensionless) |
| ε_{dup} | downcomer gas holdup at the upper part of ALC-S (dimensionless) |
| ε_o | overall gas holdup (dimensionless) |
| ε_r | riser gas holdup (dimensionless) |
| ε_{gs} | top-section gas holdup (dimensionless) |
| ρ_D | dispersion density (kg/m ³) |
| ρ_G | gas density (kg/m ³) |
| ρ_L | liquid density (kg/m ³) |
| σ | surface tension (kg/s ²) |

CHAPTER 1

INTRODUCTION

1.1 General Ideas

Generally, stirred tanks have been the most common choices of reactors in many industries because of their well studied characteristics. However, they might not be the best design for biochemical application (Onken and Weiland, 1980; Popovic and Robinson, 1989; Lu *et al.*, 1994; Benyahia, 1996). One primary reason for this is that stirred tank reactors (STRs) impose high shear stress which could damage weak cells. The presence of propeller or impeller leads to the potential contamination from mechanical seals. Fabrication of STRs requires high capital investment. Moreover, the stirring often requires high energy input which might not be necessary in low viscosity fluids. These shortcomings of the STRs lead to more investigations for new designed bioreactors with improved performance. In the light of these drawbacks a pneumatic airlift contactor (ALC) has been proposed as a potential bioprocess alternative (Dussap and Gros, 1982; Sukan and Vardar-Sukan, 1987; Young *et al.*, 1991; Garcia-Calvo, 1992; Gavrilescu and Tudose, 1995; Merchuk and Berzin, 1995). Unlike common STRs, ALCs gain their popularity through the simple design with no moving mechanical parts needed for agitation which helps eliminate the danger of easy contamination through seals, or the need for complicated magnetically driven agitators, not to mention their inherent ease of construction. In a viewpoint of biological systems, ALCs also provide an additional advantage because of their relatively low shear stress than that found in STRs. As a result, the risk of cells being damaged from the shear stress can be maintained at low level. This is of particular importance in plant and animal cell systems where cells are highly sensitive to shear stress. When compared to bubble columns, the ALCs have better mixing and, actually, greater mass transfer rate under some circumstances (e.g. in some gas-liquid-solid contactors) (Akita *et al.*, 1988; Chisti, 1989; Wachi *et*

al., 1991; Akita *et al.*, 1994). This latter is possible because of the very high gas velocities which may be used in the ALCs. These attractive features of the ALCs also lead to increasing engagement in fields of environmental technology, e.g. wastewater treatment, and chemical process industry, e.g. catalytic processes.

Despite all the advantages of ALCs described above, they suffer a serious drawback due to their comparatively low gas-liquid mass transfer particularly in large scale systems (Chisti and Moo-Young, 1987). In fact, this is an important obstacle for their application in bioprocesses. In order to improve the mass transfer performance of ALCs, it is significant to thoroughly understand their hydrodynamic and mass transfer behavior in various design configurations. However, the ALC is a relatively new system and most of the works done on ALCs were only carried out during the last two decades (Kemblowski *et al.*, 1992; Godo *et al.*, 1999). The areas of interest were various, and all of the works in the literature have limited their investigation within a specific range of operating conditions. This leads to difficulties in generalizing the system in terms of the effects of design parameters on the system performance.

The aim of this work is to narrow down these obscures by investigating hydrodynamic and oxygen mass transfer behavior in new configurations of ALCs, i.e. a vertically split draft tube ALC, and those that are coupled with baffles.

1.2 Objectives

This work is set out to:

1. Investigate the effect of design configurations on hydrodynamic behavior of ALCs
2. Investigate the effect of design configurations on gas-liquid mass transfer in ALCs.

3. Construct an empirical mathematical model that is capable of predicting hydrodynamic behavior and mass transfer phenomena in ALCs.

1.3 Scopes of Work

1. The investigation is confined to the internal-loop ALCs. The operating condition is largely limited by the capability of the employed air compressor unit which only produces air at flowrate ranging from 0.11×10^{-3} to 0.54×10^{-3} m³/s ($0.015 < U_{sg} < 0.08$ m/s). This range of operating condition is relatively reasonable for most of the application of ALCs particularly on the biochemical field (Lin *et al.*, 1976; Margaritis and Sheppard, 1981; and Zhao *et al.*, 1994)
2. Various design configurations include
 - Conventional internal-loop ALC
 - ALC with vertically split draft tube
 - ALC with baffles

Dimension of these systems are given in Section 3.1.

3. The investigation on hydrodynamic is performed with air-water system with the assumption that the liquid is Newtonian.
4. The investigation on mass transfer is based on the assumptions that the liquid phase is well mixed and oxygen concentration in gas phase is constant along the column height.

สถาบันวิทยบริการ
จุฬาลงกรณ์มหาวิทยาลัย

CHAPTER 2

BACKGROUNDS

2.1 Airlift Contactor: Anatomy

2.1.1 Classification

There have been several configurations of ALCs proposed in the literature which may be classified by various criteria (Chisti and Moo-Young, 1987; Merchuk and Siegel, 1988; Kawase *et al.*, 1994; Freitas and Teixeira, 1998). However, in this work they are categorized into two groups as follows.

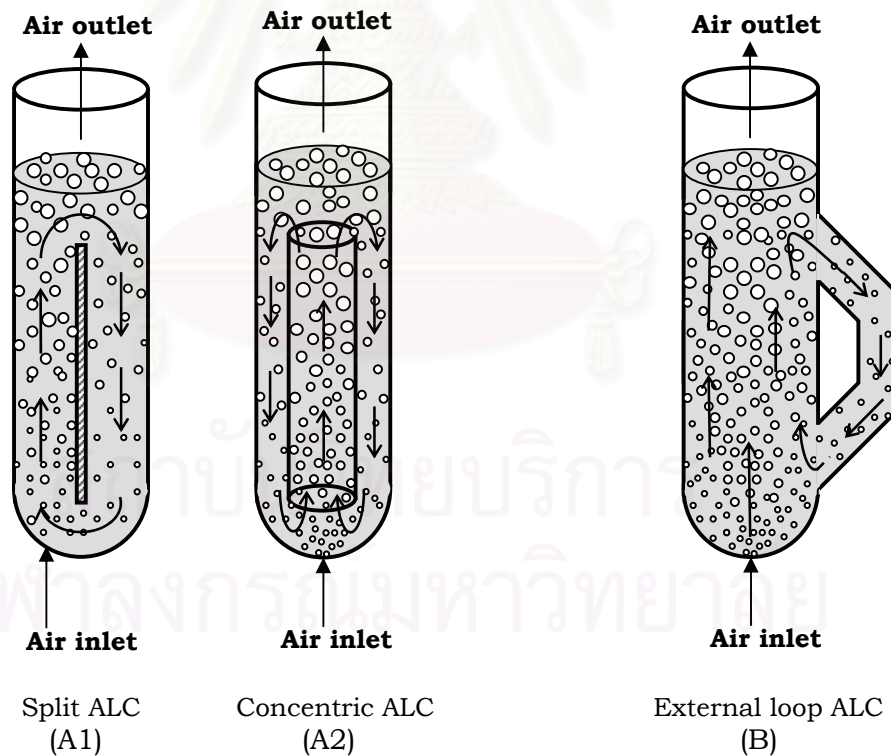


Figure 2.1 Airlift contactors: (A1) and (A2) are internal-loop airlift contactors and (B) is external-loop airlift contactor.

- i) The internal-loop ALC which is a simple column separated into two partitions. Figure 2.1 shows different designs of the internal loop ALCs: Figure 2.1 (A1) on the left hand side is the split ALC where the column is separated by a vertical baffle; and the concentric tube ALC (A2) where a concentric tube is centrally installed into the column similar to a shell and tube design.
- ii) The external-loop ALC which is constructed of two separate columns connected by horizontal section as shown in Figure 2.1 (B).

2.1.2 Transport mechanisms in ALCs

The ALC comprises three connecting zones: riser, gas separator, and downcomer as depicted in Figure 2.2, each of which is described below (Chisti, 1989).

- i) The riser is the section where gas is usually sparged creating low density fluid. This leads to the difference in fluid density between the riser and the downcomer, both liquid and gas in this section are therefore moving upwards. The riser can be represented as a bubble column with a fixed liquid flow pattern (upwards).
- ii) The gas separator is the section at the top of contactor, connecting the riser and the downcomer zones. The gas in this section disengages from the dispersion at the fluid surface totally or partially. This zone has a flow pattern similar to that of a continuous stirred tank. This highly turbulent section has a significant role in liquid mixing and gas recirculating.
- iii) The downcomer is the section where the liquid flows down from top to bottom of the contactor. Fluid in this zone has low gas holdup because a large portion of gas has already disengaged from the fluid in the gas

separator. Thus this fluid is heavier than that in the riser and therefore is moving downwards.

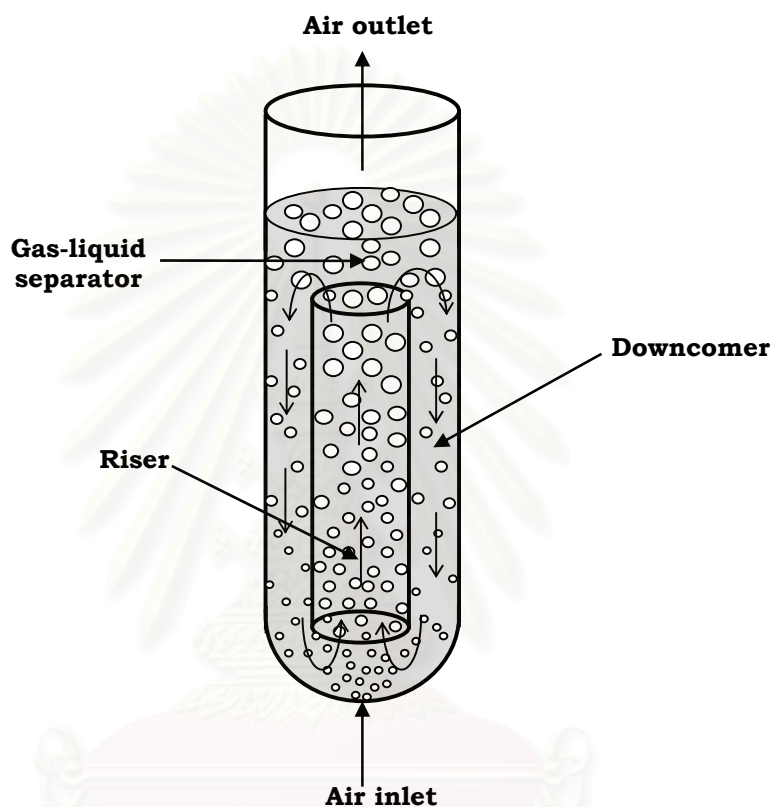


Figure 2.2 Basic structure of the airlift contactor

The behavior of the ALC is caused by the interaction of these three sections. Therefore it is necessary to consider the specific characteristics of each section in the ALC (for the design and scale up of this system).

2.2 Background: Hydrodynamic Behavior of ALCs

Since hydrodynamics play an important role in controlling the performance of ALCs, they have been extensively studied. One of the first investigations was carried out by Merchuk and Stein (1981) who studied the

gas holdup and liquid velocity using two different types of spargers, i.e. single orifice sparger and multiple orifice sparger, in an external-loop ALC. They found that the multiple orifice sparger produced a higher mean gas holdup than that in the single orifice sparger. Similarly, Merchuk *et al.* (1998) recently analysed how sparger design affected gas holdup and liquid velocity in a concentric-tube airlift bioreactor with sea water as the liquid phase. They found the different performance between cylindrical spargers and plane spargers with the same porosity, i.e. the cylindrical spargers distributed the bubbles radially as well as axially, while the plane spargers only distributed the bubbles axially. Thus, the distribution of gas obtained with cylindrical spargers was more homogeneous leading to decreasing coalescence. In addition, since the surface area of the cylindrical spargers was almost twice that of the plane spargers so they produced more bubbles.

The effect of geometrical parameters on hydrodynamics was one of the interesting factors for investigators especially in the process design field. Most of the investigations focused on the effect of the ratio between cross sectional areas of downcomer to riser (A_d/A_r) (Koide *et al.*, 1984; Weiland, 1984; Bello *et al.*, 1985; Popovic and Robinson, 1989; Choi and Lee, 1993; Gavrilescu and Tudose, 1998; and Korpijarvi *et al.*, 1999). Their results were important for the basic understanding of ALC behavior. In general, it can now be concluded that the circulation velocity in the riser increases significantly with increasing A_d/A_r . The riser gas holdup decreases as A_d/A_r increases. The reason is that when the gas bubbles in the riser move up faster, their residence time in the contactor is reduced resulting in a decrease in riser gas holdup.

Several researchers carried out the investigation on the influence of gas-liquid separator designs such as geometry, liquid height, and unaerated liquid height on ALC performance. Bentifraouine *et al.* (1997a) studied the effect of the height of the external-loop ALCs on gas holdup and liquid circulation velocity. They found that the increase of the height of the ALC (the liquid volume increased) caused a reduction in the downcomer gas holdup, and therefore

significant enhancement of liquid circulation velocity was observed. However, it was also stated that the increase in liquid circulation velocity resulted in a slight decrease of bubble residence time in the riser, and consequently a fall in overall gas holdup. Kawalec-Pietrenko and Holowacz (1998) obtained the same results with a rectangular airlift reactor. As far as the literature is concerned, there are no records of work in this area carried out for internal-loop airlift columns, except for some that have been contributed to the study of three-phase internal-loop airlift systems. For instance, Russell *et al.* (1994) analysed effects of the height of draft tube (the liquid volume was varied by the height of draft tube) on overall gas holdup, liquid circulation velocity, and mixing time in a concentric airlift fermentor which was used to cultivate the yeast *Saccharomyces cerevisiae*. The results revealed that both liquid circulation velocity and mixing time increased with increasing draft tube height, whilst the overall gas holdup was unaffected by the height of draft tube. As the passage of gas bubbles through the liquid column became more rapid with increasing liquid circulation velocity, gas residence time decreased. At the same time, however, increasing rate of liquid circulation tended to draw more bubbles into the downcomer section, thus increasing the fraction of gas recycled. These two trends had opposing effects on the magnitude of the overall gas holdup resulting in a net effect of apparently negligible change in overall gas holdup with increasing vessel height.

The effect of the unaerated liquid height (Figure 3.1) on the ALC performance was performed by Siegel *et al.* (1986) where it was found that the gas recycle rate increased with the liquid level above the draft tube in a rectangular cross-sectional airlift reactor. Bentifraouine *et al.* (1997b) studied the effect of unaerated liquid height on liquid circulation velocity in external-loop ALCs. They reported that the increase of unaerated liquid level caused a decrease of gas recirculation in the downcomer and enhanced the hydrostatic pressure driving force acting on liquid circulation velocity. Similar to the work on the effect of column height, no work in this area has been carried out for concentric tube internal-loop ALCs, except for some that have been contributed

to the study of three-phase airlift reactors. Russell *et al.* (1994) analysed effect of unaerated liquid height (the distance of unaerated liquid height above draft tube ranging from 0-0.63 m) on liquid circulation time and gas holdup in a concentric tube airlift reactor. The results indicated that gas holdup and liquid circulation time did not change with the unaerated liquid height. However, they suggested that there were two distinct zones within the top-section (or gas-liquid separator) of the airlift reactor and the bulk of the recirculating liquid was believed to flow only through a lower region. Therefore they further suggested without proof that only if the height of the unaerated liquid level was lower than the height of the lower zone then the liquid height would have an effect on the gas holdup and liquid velocity. However, work that was done on three phase systems might not be correctly applied to the two-phase because of the considerable difference between their hydrodynamic behavior.

Koide *et al.* (1984) investigated the effect of bottom clearance in concentric tube ALC. They found that the flowrate of circulating liquid increased with increasing ratio between bottom clearance and draft tube diameter (L/D_{DT}). This was because the pressure decreased with increasing bottom clearance at low L/D_{DT} . However, at high L/D_{DT} , the increase in bottom clearance had almost no effect on circulating liquid flow rate. Therefore, further increase in bottom clearance would not have effect on pressure at the bottom. The effect of bottom clearance on riser gas holdup was also investigated by Merchuk *et al.* (1994) where the bottom clearance was ranging from 0.01-0.08 m. It was found that riser gas holdup increased as the bottom clearance decreased. This was because the liquid velocity was restricted by pressure drop at the bottom. The decrease in liquid velocity led to long residence time of bubbles in the riser enhancing an increase in gas holdup. Couvert *et al.* (1999) investigated this effect in a rectangular airlift reactor and they varied the bottom clearance between 0.15 to 0.35 m. They found that the bottom clearance did not influence the global gas holdup. The reason might be that their bottom clearances were too large to have the influence on pressure.

Other works which have received considerable attention were the investigations of the performance of airlift reactors compared to bubble columns (Weiland and Onken, 1981; Bello *et al.*, 1985; Chisti and Moo-Young, 1988; and Choi and Lee, 1993). They all found that the largest gas holdup was obtained in the bubble column (BC) which was beneficial for the mass transfer performance. Weiland and Onken (1981) suggested that, despite lower mass transfer rate, the airlift reactor had advantages over the BC with regard to mixing time, longitudinal dispersion, and heat transfer. To enhance the mass transfer in airlift reactors, the modifications of airlift reactors have been suggested. Two split-cylinder airlift tower was introduced by Orazem and Erickson (1979). They revealed that two split-cylinder airlift towers produced higher gas holdup than that in single split-cylinder airlift tower at high superficial gas velocity. They explained this phenomenon that, at high superficial gas velocity, there might be more coalescence in the single split-cylinder airlift tower, causing the bubble to increase in size and to escape more quickly from the column. This led to lower gas holdup in the single split-cylinder airlift tower. Chen *et al.* (1997) introduced a novel rectangular airlift reactor with mesh baffle-plates. They found that the mesh baffle-plates had slight effect on gas holdup when compared to BC, but it had a higher gas holdup in comparison with rectangular airlift reactor. The static mixers was introduced by Gavrilesco *et al.* (1997) and they concluded that the new external-loop airlift reactor with static mixers in the riser provided a higher riser gas holdup than that in a conventional airlift reactor. They demonstrated that the presence of static mixers diminished bubble coalescence due to their shear effect resulting in a decrease in an average size of bubbles. As a consequence, the residence time of gas bubble increased, and hence the riser gas holdup increased. However, shear effect is not desirable in many applications particularly in biochemical industries. Tung *et al.* (1998) proposed a multiple draft tubes ALC and it was found that the number of bubbles in the proposed ALC were significantly increased. Consequently, the gas holdup in this new configuration was greater than that in the BC.

2.3 Background: Mass Transfer of ALCs

The data published in the literature for mass transfer in ALC varied greatly. This variation can be explained by differences in geometrical designs such as A_d/A_r . Choi and Lee (1993) studied the effect of A_d/A_r on volumetric mass transfer coefficient in external-loop airlift reactors. It was found that an increase in A_d/A_r lowered down the k_La value, and the riser gas holdup decreased due to an increase in circulation liquid velocity as A_d/A_r increased. Hence, k_La increased with decreasing A_d/A_r . These were in agreement with the works of Bello *et al.* (1985) and Al-Masry and Abasaeed (1998). Hsiun and Wu (1995) investigated the effect of A_d/A_r by varying both draft tube and column diameters. They found that in small columns (9 and 13 cm. diameters), k_La increased with decreasing A_d/A_r . On the other hand, the effect of A_d/A_r seemed negligible in large columns (19 and 29 cm. diameters). Kawalec-Pietrenko and Holowacz (1998) investigated the effect of reactor height on mass transfer in a rectangular draft tube airlift. The results revealed that k_La decreased with increasing reactor height due primarily to a decrease in gas holdup. Koide *et al.* (1983) studied the k_La value in draft tube sparged and annulus sparged airlift reactors comparing with that in BC. They found that the k_La in the draft tube sparged and annulus sparged airlift reactors were much larger than those in BC when a liquid with frothing ability was used. This was because the small bubbles were entrained into the draft tube by the circulating liquid flow. Therefore, the specific gas-liquid interfacial area in the column with draft tube might be larger than that in the BC. The effect of the gas-liquid separator design on the mass transfer performance of split-channel airlift reactors were carried out by Choi *et al.* (1995). Three configurations were investigated: a basic internal-loop head region without special features for gas-liquid separator; and two configurations with different arrangement of the upper prism. They found that the volumetric mass transfer value in the internal-loop head region without special features was the greatest because this configuration produced the largest value of the overall gas holdup.

However, some previous works indicated that gas-liquid mass transfer in ALC was comparatively low compared to BC (Chisti and Moo-Young, 1988; Wu and Jong, 1994; Tung *et al.*, 1998). Attempts have been focused on the improvement of mass transfer performance of ALCs. For instance, Lin *et al.* (1976) placed slanted baffles in an airlift fermentor and it was observed that the presence of baffles enhanced the $k_L a$ value. They explained that the slanted baffles broke the large air bubbles into smaller ones and, hence, increased the interfacial area (a). Moreover, these baffles facilitated the turbulent condition which provided relatively high value of k_L . Orazem and Erickson (1979) proposed two split-cylinder airlift tower. They found that the oxygen mass transfer was improved in the two split-cylinder airlift tower in comparison with the single split-cylinder airlift tower at large superficial gas velocity, but at low superficial gas velocity, the single and two split-cylinder airlift towers had equivalent mass transfer. It was demonstrated that, at high superficial gas velocity, the two split-cylinder airlift tower had higher gas holdup than that in the single split-cylinder airlift tower. This led to greater specific gas-liquid interfacial area in the two split-cylinder airlift tower. A double draft tube airlift fermentor was investigated by Margaritis and Sheppard (1981). They found that the addition of double draft tube into internal-loop airlift fermentor could raise the value of $k_L a$ to be higher than that in a bubble column. Stejskal and Potucek (1985) introduced a motionless mixer into an internal-loop ALC. They found that the presence of the motionless mixer produced higher value of mass transfer coefficient than that in the conventional ALC. This was because an increase in a residence time of bubble in the system with the motionless mixer resulted in an enhancement of specific gas-liquid interfacial area (a). Bando *et al.* (1992) proposed an ALC with a perforated draft tube. The results revealed that this configuration was more effective in increasing the volumetric mass transfer coefficient than that in the conventional ALC. This was due to an increase in bubble subdivision. Zhao *et al.* (1994) introduced perforated plates into a BC and an internal-loop ALC to enhance gas-liquid mass transfer for highly viscous Newtonian and non-Newtonian liquids. However, it was reported that the value of overall mass transfer coefficient ($k_L a$) depended on the trade-off

between an increase in the specific area, a (due to the breakup of bubble at perforated plates) and a decrease in mass transfer coefficient k_L (due to lower liquid velocity). Karamanev *et al.* (1996) proposed an airlift reactor with a semipermeable draft tube through which liquid could penetrate but not the gas bubbles. The results revealed that this modified reactor had a higher $k_L a$ than a conventional airlift reactor (no theoretical backup was given in this short communication). However, this permeable draft tube is not always available or feasible for several applications, i.e. those with particles deposited on the wall of the contactor. Chen *et al.* (1997) introduced mesh baffle-plates into a rectangular airlift reactor. They found that at low superficial gas velocity, the performance of the proposed airlift reactor was not different from a BC. However, at high superficial gas velocity, the mesh baffle-plates broke up large bubbles into small ones. This resulted in higher $k_L a$ in the proposed airlift reactor than that in the BC. Bang *et al.* (1998) studied gas-liquid mass transfer in the three-phase stirred airlift reactor by adding mechanical agitation inside draft tube at the bottom part. They found that mechanical stirring resulted in an importance increase of $k_L a$. Although this new configuration gave the better $k_L a$, it should be noted that the stirring might have bad influence in some applications such as cultivation of cell culture. A multiple draft tubes ALC was proposed by Tung *et al.* (1998) and it was demonstrated that this new configuration always resulted in a higher rate of gas-liquid mass transfer than that of BC. This, however, only applied to pilot scale reactors where it was possible to install multiple draft tubes in the outer column.

Although several investigations have been performed, the mass transfer performance of the ALC is still not significantly improved. This work therefore is aimed to examine the performance of new designed ALCs.

CHAPTER 3

EXPERIMENT

3.1 Experimental Equipment

The ALC employed in this work was made of clear acrylic plastic in which it was possible to observe the on-going phenomena. Attached to the outer column of the ALC were a series of measuring ports for pressure drop measurement (Figure 3.1). The measuring ports also allowed easy injection of color tracer for the liquid velocity measurement. The volumetric mass transfer was determined by using the dissolved oxygen (DO) probe. Air was sparged into the contactor by air pump and air flowrate was controlled by calibrated rotameter.

Three configurations with the same ratio between downcomer and riser cross sectional areas (A_d/A_r) of internal loop ALCs were investigated: conventional ALC; ALC with baffles in the riser (ALC-B); and ALC with a vertically split draft tube (ALC-S). A schematic representation of these contactors is given in Figure 3.2.

The three ALCs were equipped with a draft tube of the same dimensions as indicated in Table 3.1. For the ALC with baffles (ALC-B), three circular plates with 6.5 cm. diameter were placed inside the draft tube and they divided the draft tube into four equivalent sections. Each baffle plate was provided with eight 3 mm. diameter holes to reduce a dead zone occurring over the baffle. The vertically split draft tube in the last configuration (ALC-S) had the same height as the conventional straight cylindrical draft tube but was separated at the middle with the distance between the top and bottom sections of 5 cm. The sparger used in ALC, ALC with baffles, and vertically split ALC was a ring type with fourteen 1 mm. diameter holes. However, in vertically split ALC there were two spargers installed: one at the bottom and the other

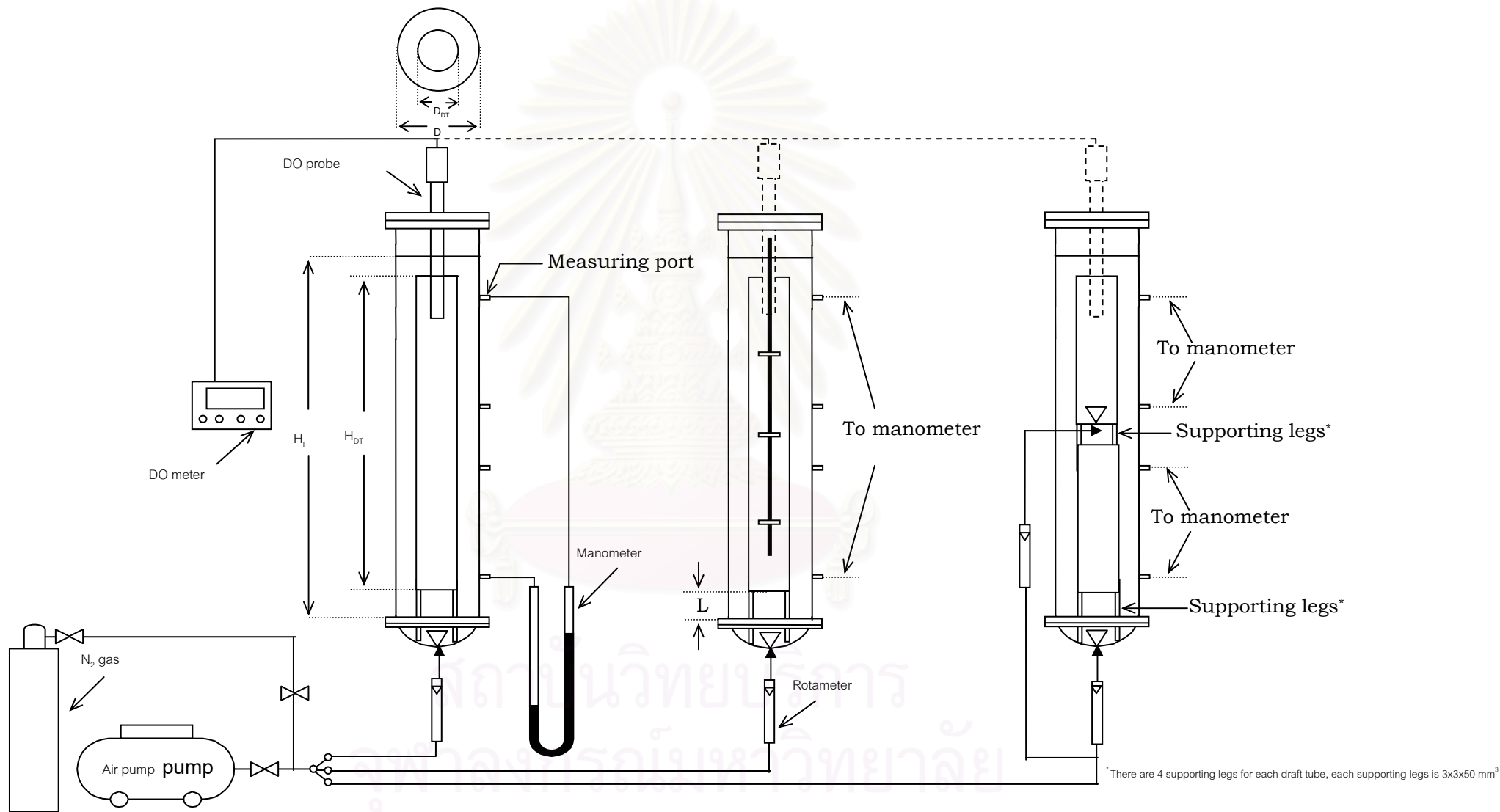


Figure 3.1 Experimental setup of the airlift contactor

at the middle of draft tube as shown in Figure 3.2. Detailed dimensions of the employed ALCs are given Figure 3.3.

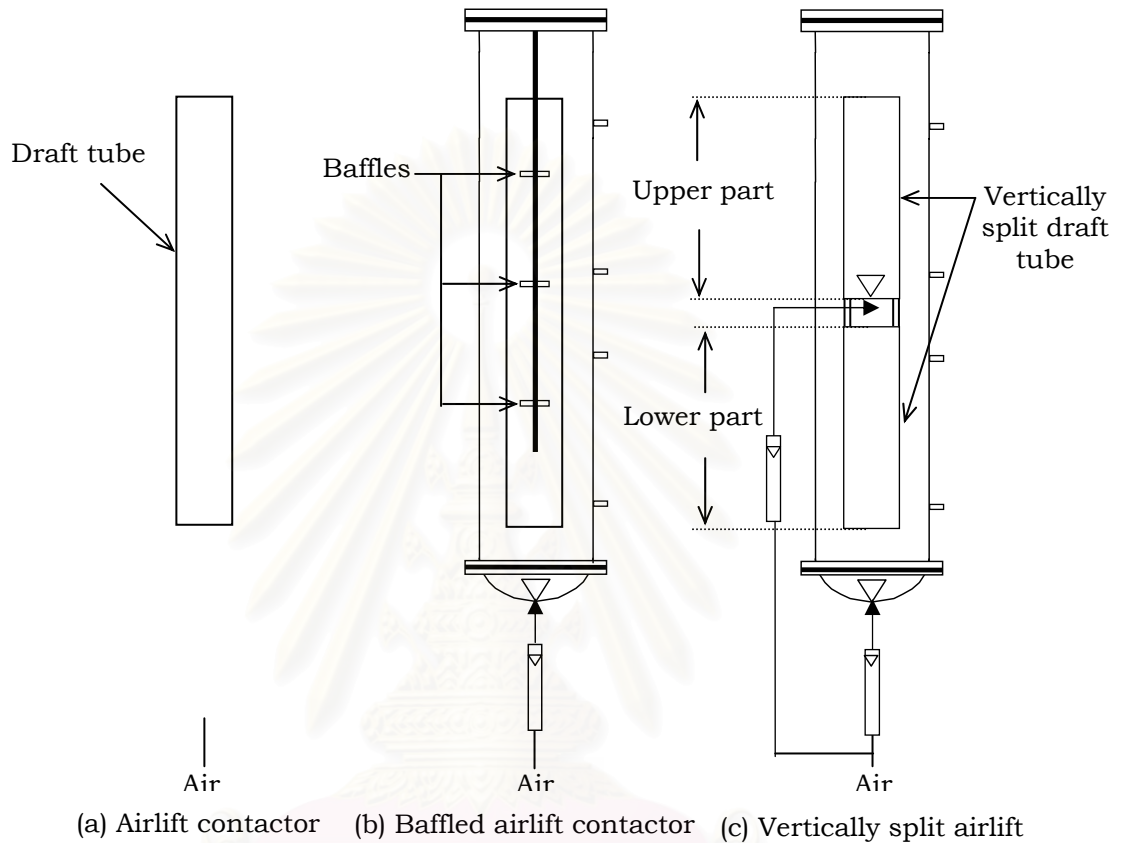


Figure 3.2 The configurations of airlift contactor employed in this work

Table 3.1. Dimensions of the employed airlift contactors.

| Column dimensions | | | ALC | ALC with baffles | Vertically split ALC |
|--------------------------|------------|-------------------|-------|------------------|----------------------|
| Diameter | (D) | (m) | 0.17 | Same | Same |
| Draft tube diameter | (D_{DT}) | (m) | 0.093 | Same | Same |
| Un-aerated liquid height | (H_L) | (m) | 1.045 | Same | Same |
| Draft tube height | (H_{DT}) | (m) | 1 | Same | Same |
| Bottom clearance | (L) | (m) | 0.015 | Same | Same |
| Nominal volume | | (m ³) | 0.016 | Same | Same |
| A_d/A_r | | (-) | 1.01 | Same | Same |
| Symbols | | | ALC | ALC-B | ALC-S |

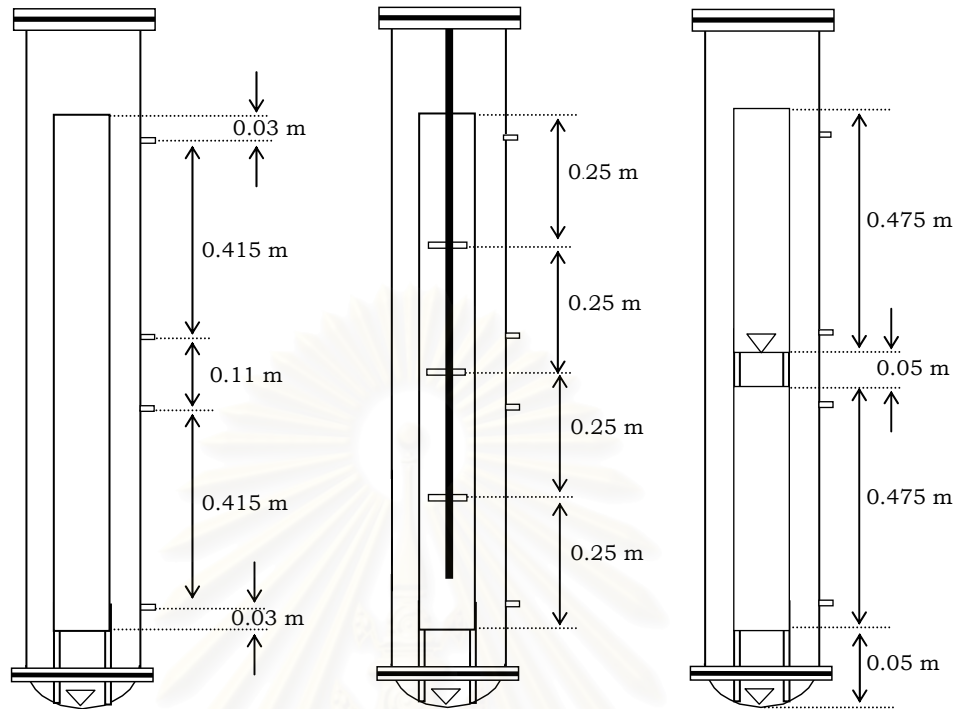


Figure 3.3 Dimensions of airlift contactors employed in this work

3.2 Experimental Procedure

Experiments were carried out as follow:

1. Calibrate a rotameter by using replacement of air in water.
2. Fill water into a contactor until water being 0.03 m. above the draft tube.
3. Sparge air into the contactor by opening pump valve. Then adjust air flowrate to $0.111 \times 10^{-3} \text{ m}^3/\text{s}$ using the rotameter and wait until the system reaches steady state.
4. Read a value of liquid dispersion height to determine the overall gas holdup (see Section 3.3.1).

5. Determine the downcomer gas holdup by measuring the pressure difference between two measuring ports located along the height of the column. This is done by connecting a manometer into two separate ports and read the difference of liquid height in the manometer.
6. Determine downcomer liquid velocity by injecting color tracer rapidly via the top measuring port of the column, then measure times required by the tracer to flow between two fixed points along the column.
7. Determine gas-liquid mass transfer coefficient by immersing a dissolved oxygen probe (DO probe) in riser at the distance of 0.16 m. below the top of draft tube. After that, purge nitrogen gas into the contactor to remove the dissolved oxygen in water. Wait until the oxygen concentration in the liquid becomes zero, stop the nitrogen feed, and sparge air into the system at the same flow rate as Step 3. Then measure time and read the DO value every ten seconds until the value of DO is constant. Calculate the mass transfer coefficient according to the calculation in Section 3.3.3.
8. Repeat the experiment (from Steps 3 to 7) at various air flowrates, i.e. 0.204×10^{-3} , 0.272×10^{-3} , 0.307×10^{-3} , 0.408×10^{-3} , 0.457×10^{-3} and 0.537×10^{-3} m³/s.
9. Repeat the experiment (from Steps 3 to 8) in various configurations of ALCs, i.e. ALC with baffles and vertically split ALC. In addition, the measurements of downcomer gas holdup and liquid velocity in the vertically split ALC were separated into two sections i.e., the upper and the lower parts (Figure 3.2).

3.3 Methods of Measurement

3.3.1 Measurement of Gas Holdups

The overall gas holdup was measured using the volume expansion method where the dispersion height, H_D , and the unaerated liquid height, H_L , were measured and the overall gas holdup, ε_o , was calculated as follows.

$$\varepsilon_o = \frac{H_D - H_L}{H_D} \quad (3.1)$$

The downcomer gas holdup, ε_d , was estimated by measuring the pressure difference, ΔP , between two measuring ports located along the height of the column:

$$\varepsilon_d = 1 - \frac{\Delta P}{\rho_L g \Delta h} \quad (3.2)$$

where $\Delta P = \rho_L g \Delta z$ therefore

$$\varepsilon_d = 1 - \frac{\Delta z}{\Delta h} \quad (3.3)$$

where Δz is the difference of liquid height in a manometer and Δh the distance between pressure measurement points.

The relationship between the holdups in different parts of the ALC can be written as:

$$\varepsilon_o = \frac{H_{DT} A_r \varepsilon_r + H_{DT} A_d \varepsilon_d}{H_D (A_r + A_d)} + \frac{(H_D - H_{DT})(A_d + A_r) \varepsilon_{gs}}{H_D (A_r + A_d)} \quad (3.4)$$

where ε_{gs} is the gas holdup in the gas-liquid separator and H_{DT} the draft tube height.

It was assumed that the gas holdup in the gas-liquid separator was approximately equal to that in the riser. This allowed the estimation of the riser gas holdup from the overall and downcomer gas holdups.

if $\varepsilon_{gs} \approx \varepsilon_r$, therefore,

$$\varepsilon_r = \frac{\varepsilon_o H_D (A_d + A_r) - H_{DT} A_d \varepsilon_d}{H_{DT} A_r + (A_r + A_d)(H_D - H_{DT})} \quad (3.5)$$

3.3.2 Measurement of Liquid Velocities

To measure the liquid velocities in the downcomer, the color tracer was injected rapidly via the measuring port of the column. The average time in downcomer, t_d , was measured as the time the tracer required to travel between the two points in the column. The downcomer liquid velocity, v_{Ld} , was then obtained from:

$$v_{Ld} = \frac{L_d}{t_d} \quad (3.6)$$

where L_d is the distance where tracer pass through between the measuring ports in the downcomer.

3.3.3 Measurement of Volumetric Mass Transfer Coefficient

Oxygen mass transfer was measured using the dynamic method. The DO meter (Jenway model 9300) was located in the riser to measure changes in DO in the dispersion, and the value of mass transfer coefficient, $k_L a$, was calculated from integrating the following mass transfer equation:

$$\frac{dC}{dt} = k_L a (C^* - C) \quad (3.7)$$

where C is the bulk concentration of dissolved oxygen and C^* the saturated concentration of dissolved oxygen. If C^* is assumed constant (which is a reasonable assumption for small scale systems), equation (3.7) can be integrated to

$$\ln(1 - \bar{C}) = -k_L a \cdot t \quad (3.8)$$

where

$$\bar{C} = \frac{C - C_0}{C^* - C_0} \quad (3.9)$$

and C_0 is the initial concentration of dissolved oxygen.

3.3.4 Measurement of Specific Power Input

Specific power input can be estimated from the head pressure in the column and the quantity of gas supplied to the system. The gas is assumed to be ideal and system is assumed to undergo isothermal expansion.

$$P_G = \frac{P \Delta V}{\Delta t} \quad (3.10)$$

where P_G is the pneumatic power input, P the pressure, and ΔV the volume of gas entering the system within the time interval, Δt .

Let $\frac{\Delta V}{\Delta t} = Q_G$ (3.11)

$$P = \rho_L g H_L \quad (3.12)$$

therefore,

$$P_G = \rho_L g Q_G H_L \quad (3.13)$$

where Q_G is the volumetric gas flow rate, ρ_L the liquid density, g the gravitational acceleration, and H_L the unaerated liquid height.

Let V_L be the liquid volume which is equal to $(A_d+A_r)H_L$, therefore,

$$\frac{P_G}{V_L} = \frac{\rho_L g Q_G}{(A_r + A_d)} \quad (3.14)$$



สถาบันวิทยบริการ
จุฬาลงกรณ์มหาวิทยาลัย

CHAPTER 4

RESULTS AND DISCUSSION

4.1 Effect of Specific Power Input on Hydrodynamic Behavior and Mass Transfer Performance in Airlift Contactors

4.1.1 Liquid and Slip Velocities

The effect of specific power input (P_G/V_L) on liquid velocity in the airlift contactor (ALC) is illustrated in Figure 4.1 which clearly shows that the liquid velocity increased with increasing P_G/V_L up to P_G/V_L of approximately 200 W/m³. This in effect means that the rate of momentum transfer from gas to liquid varied linearly with the amount of gas supplied.

At higher P_G/V_L , however, the liquid velocity seemed to reach a constant value independent of P_G/V_L . This was thought to be because the momentum or energy transfer from gas to liquid reached a constant value in this range (Figure 4.1).

If one considers the difference between riser and downcomer gas holdups at various P_G/V_L . Figure 4.2, makes it clear that these values were approximately constant at low P_G/V_L but they notably increased with enhancement of the power input at a high range of P_G/V_L . Normally, an increase in the difference of density between riser and downcomer (as the difference between riser and downcomer gas holdups increases) directly gives rise to a driving force of a circulating liquid resulting in a faster liquid movement. Thus from Figure 4.2, at low P_G/V_L the liquid velocity should have been constant, and at high P_G/V_L the liquid velocity should have increased. However, it was found that the measured liquid velocities (Figure 4.1) were totally opposite to the results expected from the gas holdup driving force. It was believed that the effect of the difference between riser and downcomer

gas holdups was not as significant as the influence exerted from the momentum transfer.

It is also interesting to look at the slip velocity or the difference between liquid and gas velocities in the ALC. Literature contain a number of investigations on slip velocity in the ALC. Some researchers showed that the slip velocity was constant, independent of P_G/V_L (Jones, 1985); and some said that it decreased slightly with the increase in gas holdup (Richardson and Zaki, 1954; Marrucci, 1965; Lockett and Kirkpatrick, 1975; Clark and Flemmer, 1985). A small number of researchers, though, indicated the opposite finding and reported that the slip velocity increased when the gas holdup increased (Davidson and Harrison, 1966; Snape, 1995). These relationships (for the slip velocity proposed in literatures) were employed to fit experimental data of this research, and the results are displayed in Figure 4.2. Table 4.1 summarizes the detail of correlations used in Figure 4.2.

The calculation results shown in Figure 4.3 reveals one common characteristic of slip velocity in a “bubble-swamp” system. That is the slip velocity tends to decrease slightly with increasing P_G/V_L . It might be reasonable to say that in a system where there is a swamp of bubbles, the interactions between bubbles will slightly hinder the movement of each other. This resulted in a reduction in the average bubble velocity with enhancing P_G/V_L . This result was in particularly good agreement with the finding of Merchuk and Stein (1981) who found that the slip velocity in the external-loop airlift reactor slightly decreased as the superficial gas velocity increased up to the superficial gas velocity of 0.15 m/s.

However, it is worth noting that there were reports from other investigations which found that further increase in the superficial gas velocity at high P_G/V_L gave an opposite result, i.e. the slip velocity became higher. This is possible since bubbles coalesce more easily at high superficial gas velocity and therefore the bubble terminal rise velocity increases accordingly.

Table 4.1 Expressions showing the relationship between slip velocity and other parameters

| Expression* | Source | Remark |
|--|---|---|
| $v_s = v_G - v_L$ (4.1) | Jones (1985), Choi and Lee (1990), and Calvo and Leton (1991) | $v_G = U_{sg}/\varepsilon$ $v_L = U_{sg}/(1-\varepsilon)$ |
| $v_s = u_{b\infty}(1-\varepsilon)^n$ (4.2) | Clark and Flemmer (1985) | $n = 0.702$ |
| $v_s = u_{b\infty}(1-\varepsilon)^{n-1}$ (4.3) | Richardson and Zaki (1954) | $n = 2.39$ for air-water system |
| $v_s = \frac{u_{b\infty}(1-\varepsilon)}{(1-\varepsilon^{5/3})}$ (4.4) | Marruci (1965) | For air-water system |
| $v_s = u_{b\infty}(1-\varepsilon)^{1.39}(1+2.55\varepsilon^3)$ (4.5) | Lockett and Kirkpatrick (1975) | The correlation factor $(1+2.55\varepsilon^3)$ took into account bubble deformation |
| $v_s = \frac{u_{b\infty}}{(7.5\varepsilon^2 + 1)^{1/2}}$ (4.6) | Joshi and Lali (1984) cited in Snape <i>et al.</i> (1995) | For air-water system |

* v_s slip velocity, v_G absolute gas velocity, v_L liquid velocity, U_{sg} superficial gas velocity, ε gas holdup and $u_{b\infty}$ terminal bubble rise velocity.

4.1.2 Riser Gas Holdup

The influence of P_G/V_L on the riser gas holdup is presented in Figure 4.2. One can observe from this figure that the dependence of riser gas holdup on P_G/V_L was almost linear, i.e. the riser gas holdup increased proportionally with the increase in P_G/V_L . This was not surprising as the quantity of gas entering the riser is proportional to the power input

according to Equation (3.14). This shows that increasing P_G/V_L directly increased the quantity of gas entering the riser and led to an enhancement of riser gas holdup as evidenced in the experimental results. In addition, this results agreed well with the finding in the literatures (Bello *et al.*, 1985; Siegel *et al.*, 1986; Choi and Lee, 1990; Kawase *et al.*, 1995; Merchuk *et al.*, 1996; Guo *et al.*, 1997; Korpijarvi *et al.*, 1999).

At $P_G/V_L > 200 \text{ W/m}^3$, although the experimental results still indicated a linear relationship between riser gas holdup and P_G/V_L , two opposing phenomena are expected to take place in the system: (1) a significant rate of bubble coalescence in the riser region. This resulted in a larger bubble diameter which decreased the bubble residence time; and (2) more bubbles were being carried up into the riser, consequently, the riser gas holdup increased. It was predicted that the positive effect was greater than the negative. Therefore the riser gas holdup still linearly increased with increasing P_G/V_L . This mechanism is shown graphically in Figure 4.4.

4.1.3 Downcomer Gas Holdup

Downcomer gas holdup is a result of bubbles being carried over from riser by the circulating liquid. At low P_G/V_L ($P_G/V_L < 200 \text{ W/m}^3$) the downcomer gas holdup tended to increase steadily with increasing P_G/V_L as depicted in Figure 4.3. This was due to the increase in liquid velocity when increased P_G/V_L (as explained in Section 4.1.1). It is known that bubbles can travel down the downcomer only if its terminal velocity is lower than liquid velocity. Thus more bubbles are forced to move down in the downcomer with enhancing liquid velocity, and as a result, the downcomer gas holdup increases (Chisti, 1989).

On the other hand, the same figure (Figure 4.3) shows that the rate of increase in the downcomer gas holdup had a tendency to decrease with increasing P_G/V_L at higher range of P_G/V_L . It is known that bubble rise velocity is a function of bubble size according to the following expression (Prince and Blanch, 1990).

$$u_r = \left[\frac{2.14\sigma}{\rho_L d_B} + 0.505gd_B \right]^{1/2} \quad (4.7)$$

where u_r is the bubble rise velocity, ρ_L the liquid density, σ the surface tension, g gravitational acceleration and d_B the bubble diameter.

In this case, large P_G/V_L created more turbulent condition in the ALC, and hence increased the possibility that bubbles collided and coalesced respectively. This resulted in an increasing bubble size, and also the bubble terminal velocity. Therefore the possibility of the downward movement of bubbles in downcomer decreased. This exerted a negative effect on the downcomer gas holdup. Accordingly the rate of increase in the downcomer gas holdup declined.

4.1.4 Overall Gas Holdup

The increase in P_G/V_L gave rise to the overall gas holdup. This is evidenced from experimental results as shown in Figure 4.2. With increasing P_G/V_L both the riser and downcomer gas holdups increased (Sections 4.1.2 and 4.1.3). The overall gas holdup was in fact the combination of holdups in the riser and downcomer. Therefore the increase in the riser and the downcomer gas holdups consequently led to an enhancement of the overall gas holdup.

At high P_G/V_L however, the rate of increase in the overall gas holdup tended to decrease slightly. This was due to the effect of the downcomer gas holdup whose increasing rate tended to decrease at high P_G/V_L (Section 4.1.3).

4.1.5 Mass Transfer Coefficient

Figure 4.5 suggests that the mass transfer coefficient ($k_L a$) was enhanced with increasing P_G/V_L until P_G/V_L reached the value of around 200 W/m³ after which the influence of P_G/V_L on the mass transfer coefficient

seemed to decrease slightly. The explanation follows. Increasing P_G/V_L normally resulted in two corresponding phenomena. Firstly, since increasing P_G/V_L was actually an increase in the volume of gas input to the system, the gas holdup in the system was enhanced. Provided that size of bubbles was unaltered, the increase in overall gas holdup gave a consequent rise to the specific gas-liquid interfacial area per unit liquid volume (a). Secondly, the increase in P_G/V_L resulted in a more rigorous mixing condition or what usually known as turbulence. This turbulence enhanced the liquid phase mass transfer coefficient (k_L). However, the value of k_L depended partially on the difference between gas and liquid velocities or “slip velocity” which has been found in Section 4.1.1 to be reversely influenced by P_G/V_L . Therefore the value of k_L might not significantly change with P_G/V_L , the evidence shown in Figure 4.6. Owing to these effects (higher a and constant k_L) the mass transfer coefficient increased as P_G/V_L increased.

At high P_G/V_L the effect of P_G/V_L on the mass transfer coefficient became slight negative rather than positive. This was because of the coalescence of bubbles (this will be explained in Section 4.2.5) and the reduction in the increasing rate of the overall gas holdup (Section 4.1.4) which negatively impacted the a value. As a consequence, at high P_G/V_L the influence of P_G/V_L on the mass transfer coefficient reduced (see Figure 4.5).

4.2 Effect of Baffles on Hydrodynamic Behavior and Mass Transfer Performance in Airlift Contactors

4.2.1 Liquid Velocity

Liquid velocity obtained from the experiment with ALC are plotted in Figure 4.7 together with the results from the ALC-B. The presence of baffles caused a marked decrease in the liquid velocity. This was because baffles obstructed a flow of liquid leading to the increase in a resistance to liquid flow. As a consequence, the liquid velocity in the ALC-B became lower. In addition, a decrease in the gas velocity in the ALC-B due to the energy loss from colliding with baffles resulted in a decrease in the energy or momentum

transfer from gas to liquid. Therefore the liquid velocity in the ALC-B was significantly lower than in ALC.

However, at high P_G/V_L ($P_G/V_L > 200 \text{ W/m}^3$) the liquid velocity in ALC did not markedly change with P_G/V_L (Section 4.1.1) while the liquid velocity in ALC-B still increased with P_G/V_L (Figure 4.7). One possible explanation for this was that the obstruction of baffles to the rising gas bubbles led to an enhancement of bubbles residence time. This provided extra contacting time between bubbles and liquid and also for momentum or energy transfer from gas to liquid. For this reason at high P_G/V_L the momentum transfer of gas bubble in the ALC-B still had effect on the liquid velocity.

4.2.2 Riser Gas Holdup

As depicted in Figure 4.8, the more favorable riser gas holdup was obtained in the ALC-B at low P_G/V_L ($P_G/V_L < 200 \text{ W/m}^3$). This could be attributed to the fact that bubbles lost their energy when they collided with baffles and hence, the gas velocity decreased. This resulted in an increase in the residence time of gas bubbles. Furthermore, baffles also retarded the liquid velocity as described earlier, which led to the increase in the residence time of gas bubbles. As a result, the riser gas holdup in the ALC-B was more than in the ALC.

At higher P_G/V_L , on the other hand, the increasing rate of riser gas holdup in ALC was larger than that in ALC-B causing the values of riser gas holdups in both contactors to be almost the same (Figure 4.8). This was because the reduction in the increasing rate of liquid velocity in the ALC-B with P_G/V_L was not as severe as that in the ALC (Section 4.2.1). As explained above, an increase in the liquid velocity lowered the residence time of gas bubbles. Thus the residence time of bubbles in the ALC-B had a tendency to decrease with increasing P_G/V_L . Note that the residence time of bubbles in the ALC also tended to decrease but to a smaller extent when compare to that of ALC-B.

4.2.3 Downcomer Gas Holdup

At low P_G/V_L ($P_G/V_L < 200 \text{ W/m}^3$) it is clear that the downcomer gas holdup in the ALC was greater than that in the ALC-B (Figure 4.9). This was because of the higher liquid velocity in ALC (Section 4.2.1) that resulted in more bubbles being migrated into the downcomer. In addition, the bubble size in the ALC was also smaller than in the ALC-B (this will be explained in Section 4.2.5) leading to the promotion of the downward movement of bubbles in the downcomer of the ALC.

However, at high P_G/V_L , the values of downcomer gas holdup in the ALC-B became closer to the values of downcomer gas holdup obtained in the ALC as shown in Figure 4.9. This was because at high P_G/V_L there was significant bubble coalescence in the ALC as described in Sections 4.1.2 and 4.1.3. On the contrary, in the ALC-B the effect of the bubble coalescence disappeared. It is expected that bubbles in ALC-B had already reached their maximum or “equilibrium” size, d_{Be} , and larger bubbles would breakup into smaller bubbles due to the collision with wall or other surfaces. Therefore no influence of bubble coalescence in ALC-B at higher P_G/V_L was observed.

In conclusion, bubble coalescence occurred significantly at low P_G/V_L in the ALC-B. The size of bubbles remained unaltered at its steady state value, and bubble coalescence had no influence on the performance of the contactor. In the ALC, the situation is somewhat different because bubbles seems to gradually coalesced into bigger bubbles and the equilibrium size was not seemed to be reached at the employed range of specific power input. This mechanism is shown in a diagram in Figure 4.10.

4.2.4 Overall Gas Holdup

It can be seen from Figure 4.11 that the overall gas holdup in the ALC was slightly higher than that in the ALC-B. This can be explained by looking at their gas holdups in riser and downcomer. As described in Sections 4.2.2 and 4.2.3, the riser gas holdup in the ALC-B was slightly more than that in the ALC while the downcomer gas holdup in the ALC was significantly

greater than that in the ALC-B. This resulted in a larger overall gas holdup in the ALC than in the ALC-B.

4.2.5 Mass Transfer Coefficient

Experimental results in Figure 4.12 state that at low P_G/V_L ($P_G/V_L < 200 \text{ W/m}^3$) the rate of oxygen mass transfer from gas to liquid in the ALC-B was greater than that in the ALC. This can be explained as follows.

Baffles exerted two opposing effects on gas-liquid mass transfer. Firstly, it forced the coalescence of bubbles resulting in a bigger bubble size. This reduced the gas-liquid interfacial area (a) and caused the reduction in the mass transfer coefficient ($k_L a$). To illustrate this effect, the correlation proposed by Clark and Flemmer (1985) is considered (Equation 4.8).

$$v_s = u_{b\infty} (1 - \varepsilon)^n \quad (4.8)$$

where v_s is the slip velocity, $u_{b\infty}$ the terminal bubble rise velocity of a single bubble in a stagnant liquid system and ε the gas holdup. This correlation suggests that the slip velocity was a function of the terminal bubble rise velocity and the gas holdup ($1-\varepsilon$). As explained in Section 4.1.1, in a swamp bubbles system, the interactions between bubbles will hinder the movement of each bubble which results in a reduction in the average bubble velocity. Therefore the actual bubble velocity, v_s , is slightly less than the terminal bubble rise velocity ($u_{b\infty}$).

From Figure 4.13 the best fit found for the ALC system is:

$$v_s = 0.26831(1 - \varepsilon)^{13.63} \quad (4.9)$$

The value of $u_{b\infty}$ obtained from this research, 0.2683 m/s, is in good agreement with other researchers (Merchuk and Stien, 1981; Clark and Flemmer, 1985; and Utiger *et al.*, 1999).

And for the ALC-B system:

$$v_s = 0.37524(1 - \varepsilon)^{10.736} \quad (4.10)$$

Equations (4.9) and (4.10) clearly show that the ALC-B had the terminal bubble rise velocity more than the ALC (the terminal bubble rise velocity of ALC-B was 0.37524 m/s while the terminal bubble rise velocity of ALC was 0.26831 m/s). Generally, the bubble velocity is a function of bubble diameter such that larger bubbles move faster than small ones. Therefore in this case the bubble size in the ALC-B should be larger than that in the ALC.

In conclusion it can be said that baffles facilitate bubbles coalescence which leads to an increase in bubble size and results in a decrease in “ a ”. In addition, the overall gas holdup of the ALC-B was lower than that in ALC (Section 4.2.4) which also negatively influenced the value of “ a ”.

The second effect is on the k_L value. The experiment in Figure 4.6 illustrates that the values of k_L/d_B in the ALC-B were higher than that in the ALC. As described above, the ALC-B had a larger bubble diameter (Equations 4.9 and 4.10) and had higher values of k_L/d_B (Figure 4.6), it was thereafter expected that the k_L value of ALC-B was greater than ALC. It was believed that the presence of baffles caused severe turbulence leading to an enhancement of k_L .

The resulting $k_L a$ in ALC-B was influenced by both aforementioned factors. In summary, it is thought that the effect of baffles on k_L value, rather than the effect on “ a ” value, dominated the rate of mass transfer in this system. Accordingly, the ALC-B had a favorable value of on $k_L a$.

However, the same figure (Figure 4.6) depicts that k_L in the ALC-B decreased continuously with increasing P_G/V_L . This was expected to be due to the presence of dead zones below each baffle in the system, and these dead zones became larger with increasing P_G/V_L . Accordingly, a turbulent condition as described above was faded away by these dead zones resulting

in a gradual decrease in k_L value. At $P_G/V_L > 200$ W/m³, the size of dead zone might have reached a constant value, and this was reflected in the value of k_L which became more stable. This mechanism of dead zones is illustrated in Figure 4.14.

4.3 Effect of Vertically Split Draft Tube on Hydrodynamic Behavior and Mass Transfer Performance in Airlift Contactors

4.3.1 Liquid Velocity

Figure 4.15 shows that at the same specific power input, liquid in ALC-S moved much slower than liquid in ALC. Before explaining how this took place, let us consider the following derivation.

In the ALC-S, air was supplied equally to the column at two locations: one at the bottom, and one in the middle. Therefore the specific power input to the ALC-S can be calculated from the combination of power input at the bottom and at the middle of the column (Equation 4.11).

$$\frac{P_G}{V_L} = \frac{\rho_L g Q_{G1}}{2(A_r + A_d)} + \frac{\rho_L g Q_{G1}}{4(A_r + A_d)} \quad (4.11)$$

where P_G/V_L is the specific power input, ρ the liquid density, g the gravitational acceleration, H_L the height of liquid level, and Q_{G2} the gas flow rate to the ALC-S. In addition, the first term on the right-hand-side represents the specific power input at the bottom, and the second term is for the sparger at the middle of the column.

Also recall that the specific power input of the ALC is

$$\frac{P_G}{V_L} = \frac{\rho_L g Q_{G2}}{(A_r + A_d)} \quad (4.12)$$

where Q_{G2} the gas flow rate to the ALC.

Both systems were compared based on the same P_G/V_L and hence:

$$\frac{\rho_L g Q_{G2}}{(A_r + A_d)} = \frac{\rho_L g Q_{G1}}{2(A_r + A_d)} + \frac{\rho_L g Q_{G1}}{4(A_r + A_d)} \quad (4.13)$$

Since all other parameters, i.e. $(A_r + A_d)$, ρ and g were controlled at the same level, Equation (4.13) can be reduced to

$$Q_{G2} = \frac{3Q_{G1}}{4} \quad (4.14)$$

or

$$Q_{G1} = \frac{4Q_{G2}}{3} \quad (4.15)$$

Equation (4.15) reveals that the gas flowrate to the ALC-S was four-thirds of that in the ALC. From previous results, it was expected that liquid velocity would be somewhat proportional to the gas throughput of the system, i.e. the liquid velocity in the ALC-S was greater than that in the ALC. However, it was found that in the ALC-S, the liquid velocity both in the upper and lower parts were less than the liquid velocity in the ALC. It was explained as followed. The dilemma exists as Figure 4.16 shows that at low P_G/V_L the liquid flowrate at the lower part was higher than the upper part. This result is important as it implies that liquid flowrate must have circulated in two separate loops (Figure 4.17). This is because if there was only one loop, the flowrates at various sections should have been the same. However, the interaction between these two loops were not observable from the existing experiment. Further investigation on this behavior is being conducted at the Department of Chemical Engineering, Faculty of Engineering Chulalongkorn University. Due to the occurrence of two loops in the ALC-S, it was believed that in ALC-S there exists a resistant layer between the upper and lower parts. Liquid stream when passed through this layer lost energy. This

mechanism was not taken place in the common ALC. As a result, the velocity in the ALC-S was not as high as that in the ALC.

In addition, the liquid velocity at the lower part of the ALC-S was likely to be lower than the liquid velocity in the upper part, particularly at high P_G/V_L (Figure 4.15). This was due to the fact that the gas throughput at the lower part was much less than that in the upper part. Therefore the energy transfer at the lower part of the ALC-S was smaller, and accordingly, the slower movement of liquid was obtained.

4.3.2 Downcomer Gas Holdup

As illustrated in Figure 4.9, the downcomer gas holdup at the upper part of the ALC-S was greater than in the ALC. This result implies that the introduction of vertically split draft tube increased a number of small bubbles in the system. This is because a large fraction of bubbles only had to travel half distance from the sparger to the gas separator region which therefore reduced the chance of being contacted with other bubbles. Hence, a decrease in bubble coalescence could be well observed. Consequently, the downcomer gas holdup in the ALC-S increased.

However, the downcomer gas holdup at the lower part of the ALC-S was less than that in the ALC. This was because there was less quantity of gas per unit volume at the lower part of the ALC-S, thus the quantity of gas bubble that could be drawn into the downcomer was significantly lower.

4.3.3 Overall Gas Holdup

At low specific power input the overall gas holdup in the ALC-S was more than that in the ALC (Figure 4.11). As explained in Section 4.3.2, the size of bubbles in the ALC-S was smaller than those in ALC. This resulted in a longer residence time of gas bubble than those in the ALC. (the residence time of a gas bubble was inversely dependent of its size). In addition, as described in Section 4.3.1, the liquid velocity in the ALC-S was lower than that in the ALC leading to an enhancement of the residence time of gas

bubble. These results positively influenced the overall gas holdup, and hence, the overall gas holdup in the ALC-S was higher than that in the ALC.

However, at high specific power input the increasing rate of overall gas holdup did not increase in the same speed as the rate at low P_G/V_L rather it tended to slow down. As it was described earlier that the overall gas holdup was the combination of gas holdups in riser and downcomer, and since there were not significant changes in downcomer gas holdup, the change in the overall gas holdup was expected to be the result of the holdup in the riser. That is to say that the rate of increase in riser gas holdup had slowed down at high P_G/V_L . This conclusion was made based on the rational picture of what happened in the system, and not from the experimental observation. This is because the existing configuration of the ALC-S did not allow proper measurement of various parameters in the riser.

4.3.4 Mass Transfer Coefficient

The most favorable values of the mass transfer coefficient were obtained in the ALC-S at low specific power input, the evidence shown in Figure 4.12. This can be attributed to the higher overall gas holdup which exerted the positive effect on the specific gas-liquid interfacial area (a). Moreover, as explained earlier, there was a lot of small bubbles in the ALC-S resulting in an increase in a . As a result, the mass transfer coefficient in the ALC-S was higher than that in the ALC.

However at $P_G/V_L > 150 \text{ W/m}^3$, the increasing rate of the mass transfer coefficient in the ALC-S decreased, and the value of mass transfer coefficient had a tendency to be lower than that in the ALC. This was because of the reduction of the increasing rate of the overall gas holdup (Section 4.3.3) which reduced the specific gas-liquid interfacial area " a ".

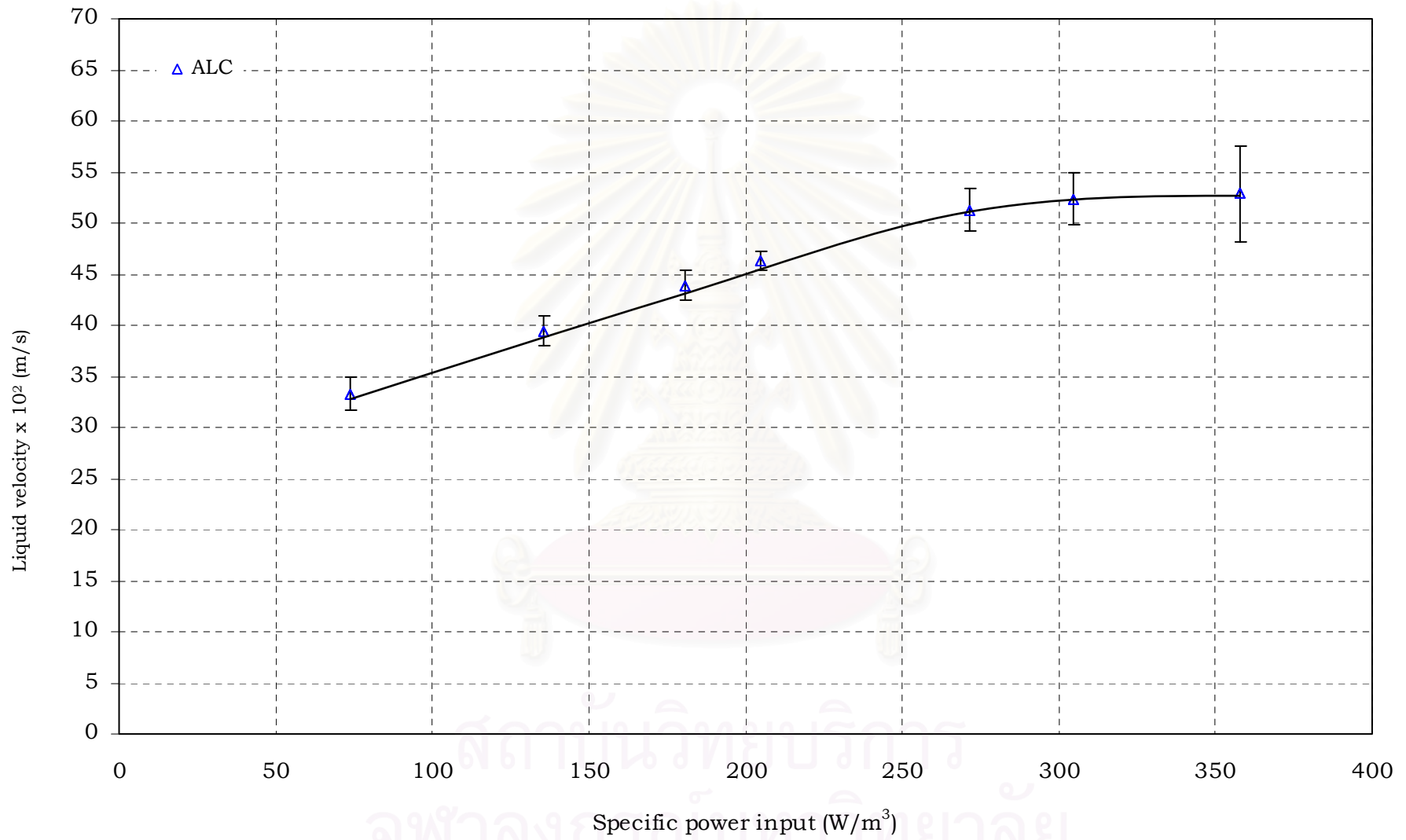


Figure 4.1 Relationship between liquid velocity and specific power input in the ALC

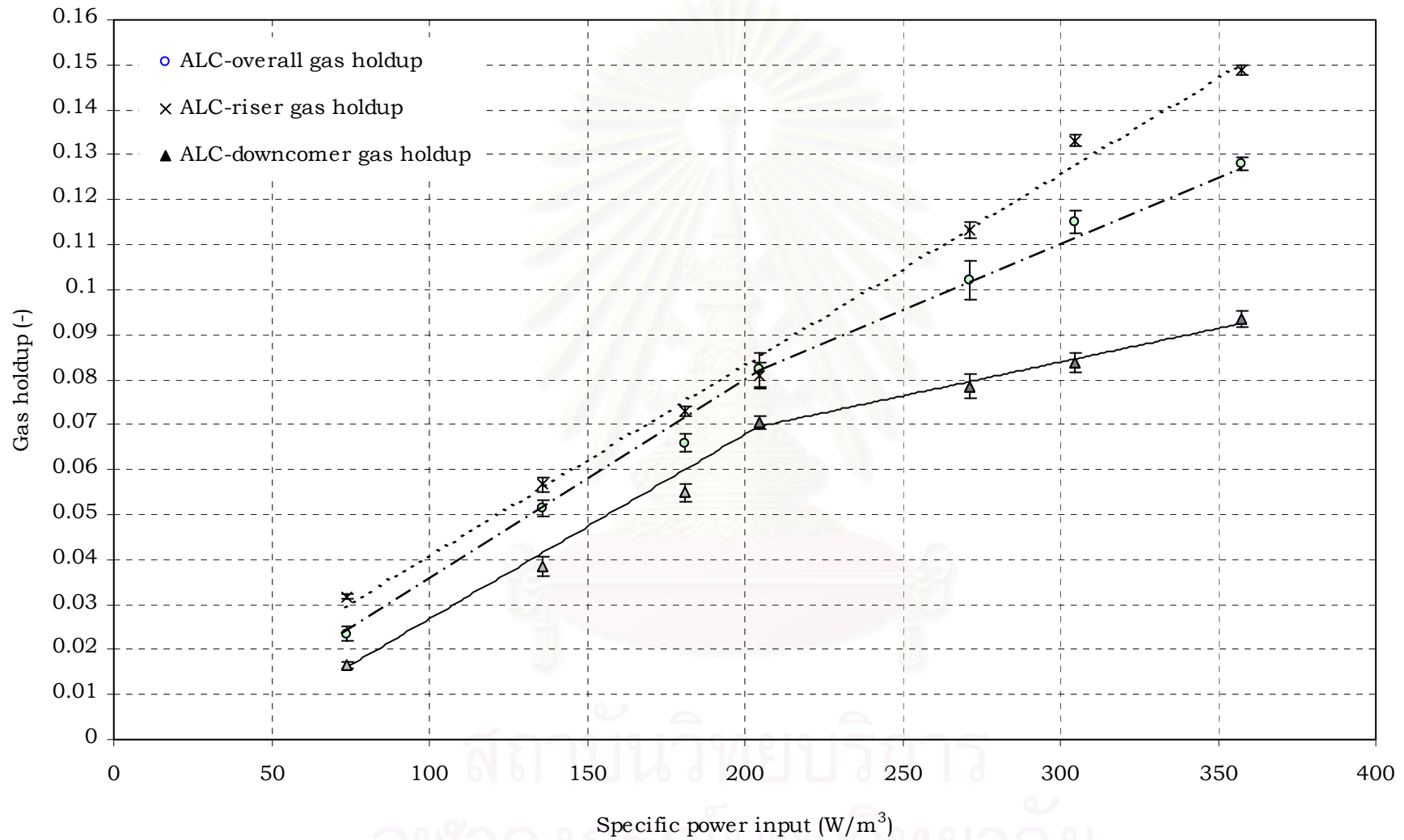


Figure 4.2 Relationship between gas holdups and specific power input in the ALCs

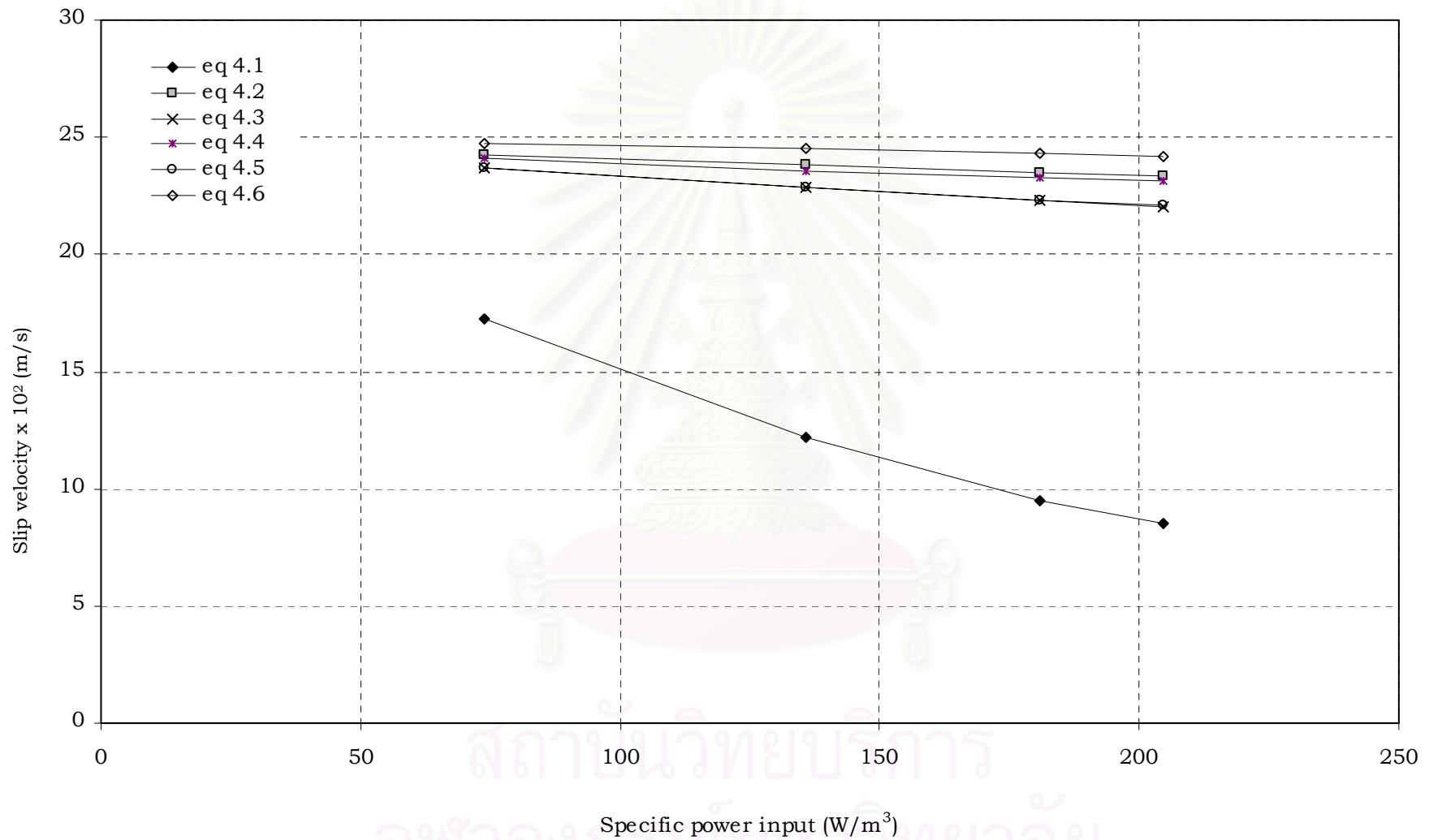


Figure 4.3 Relationship between slip velocities and specific power input in the ALC

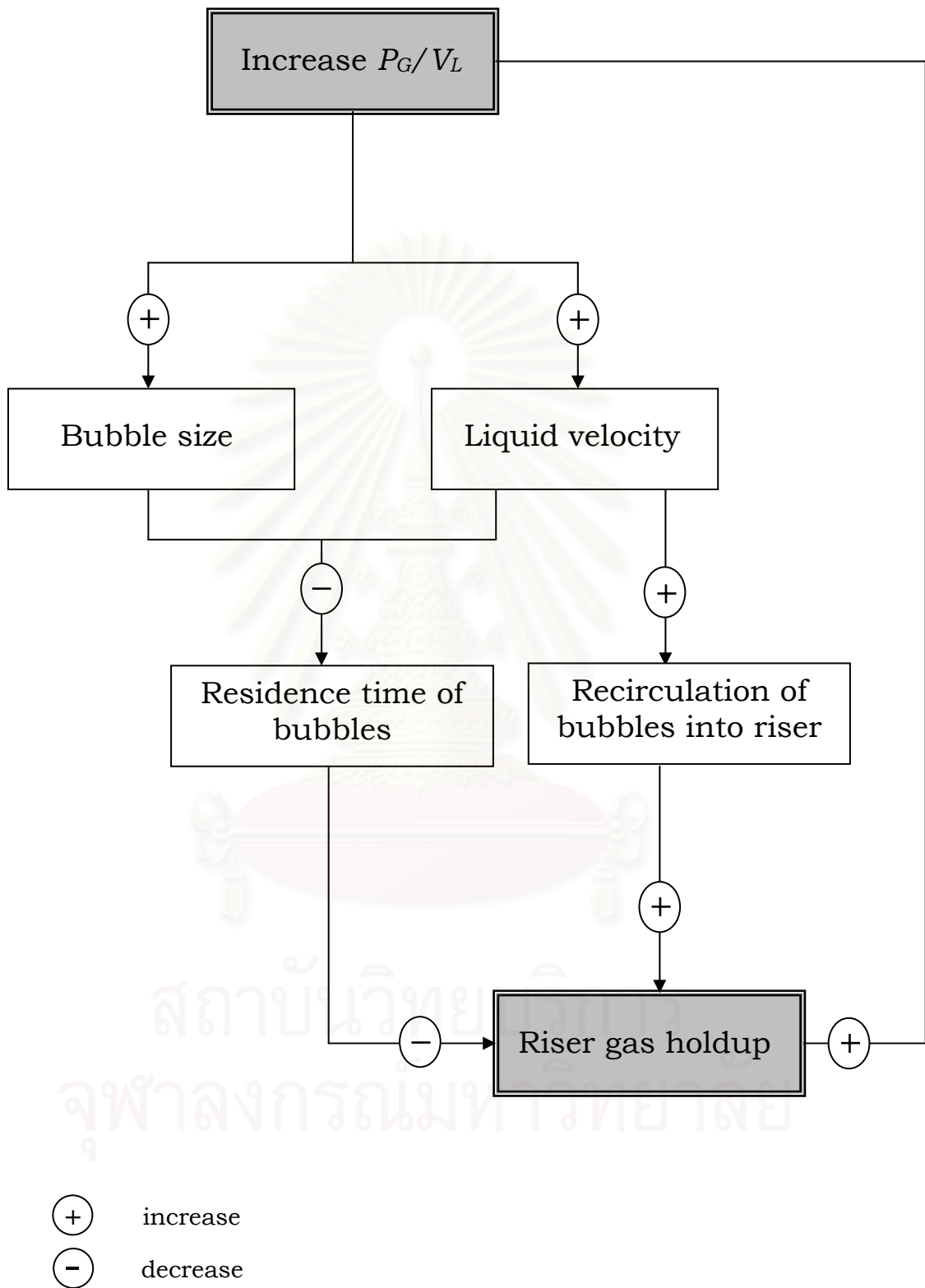


Figure 4.4 The mechanism controlling riser gas holdup

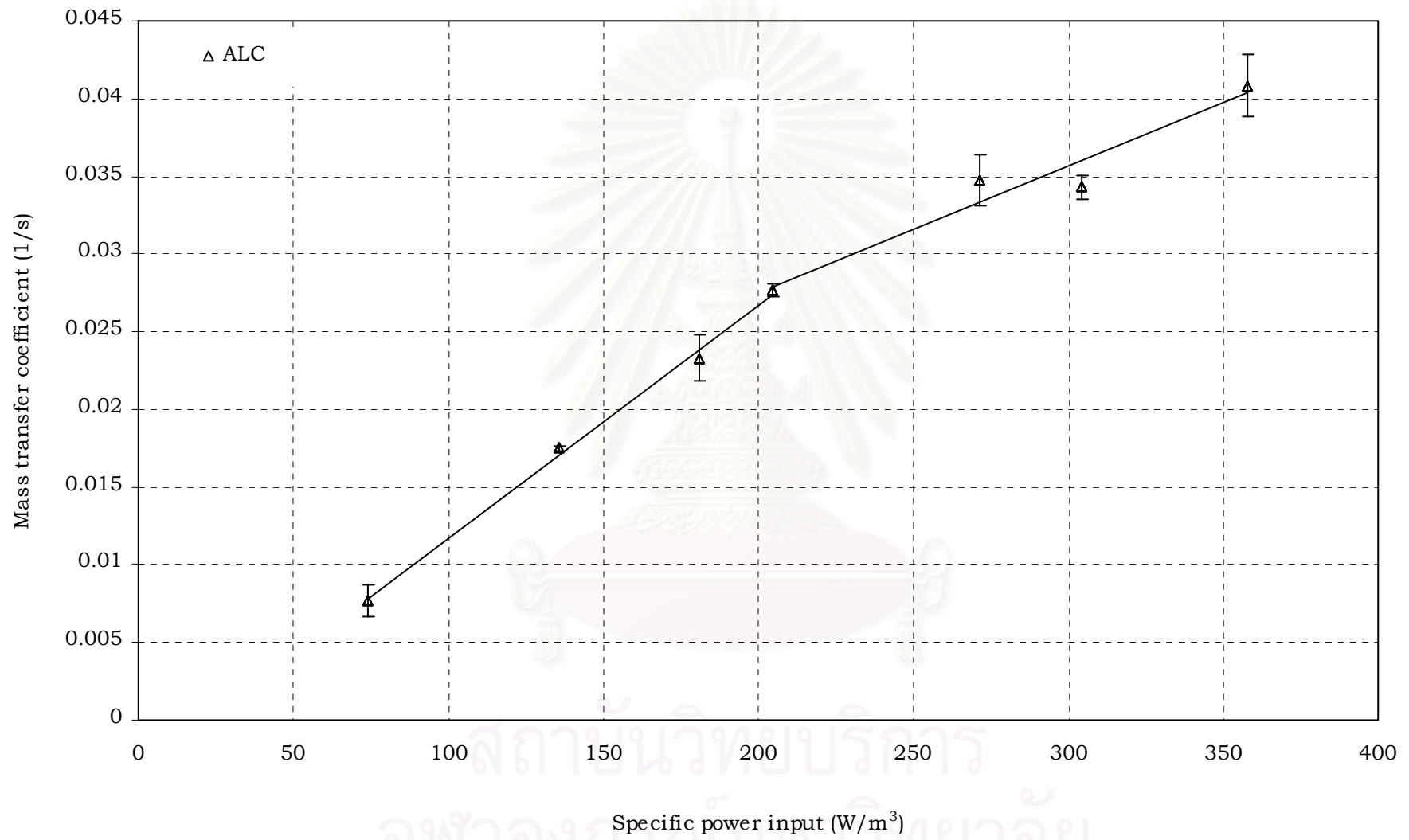


Figure 4.5 Relationship between mass transfer coefficient and specific power input in the ALC

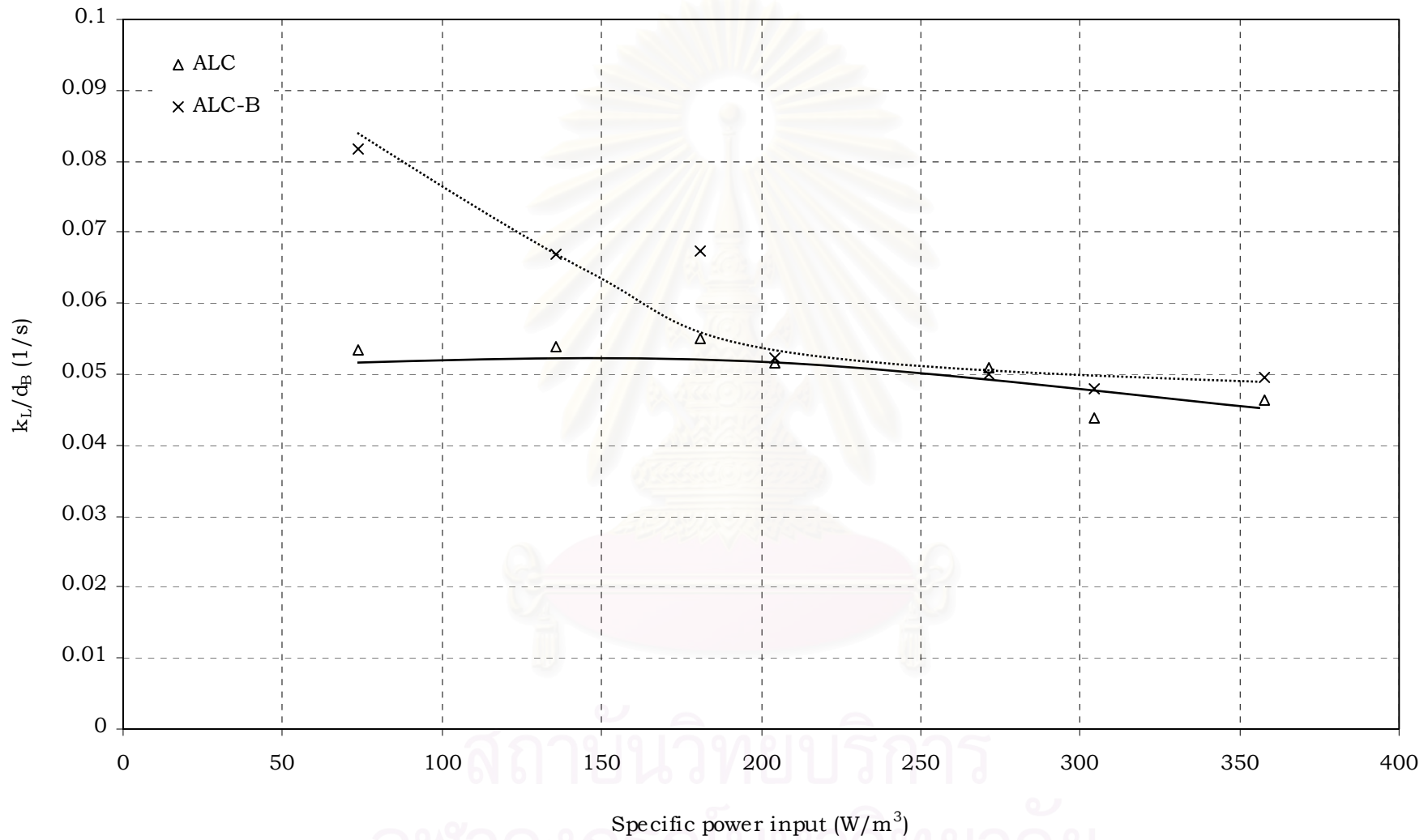


Figure 4.6 Relationship between k_L/d_B and specific power input in various configurations of ALCs

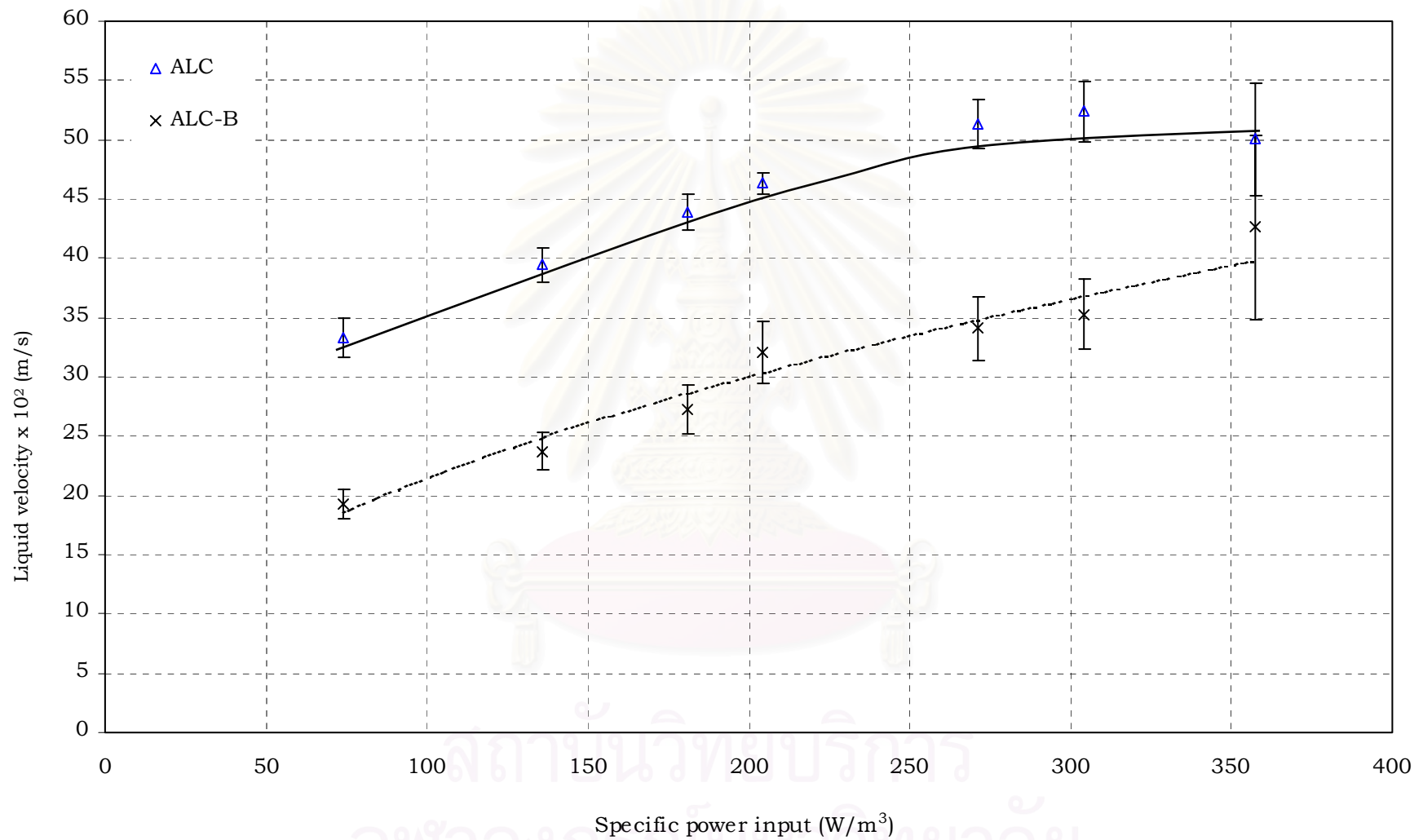


Figure 4.7 Relationship between liquid velocity and specific power input in various configurations of ALCs

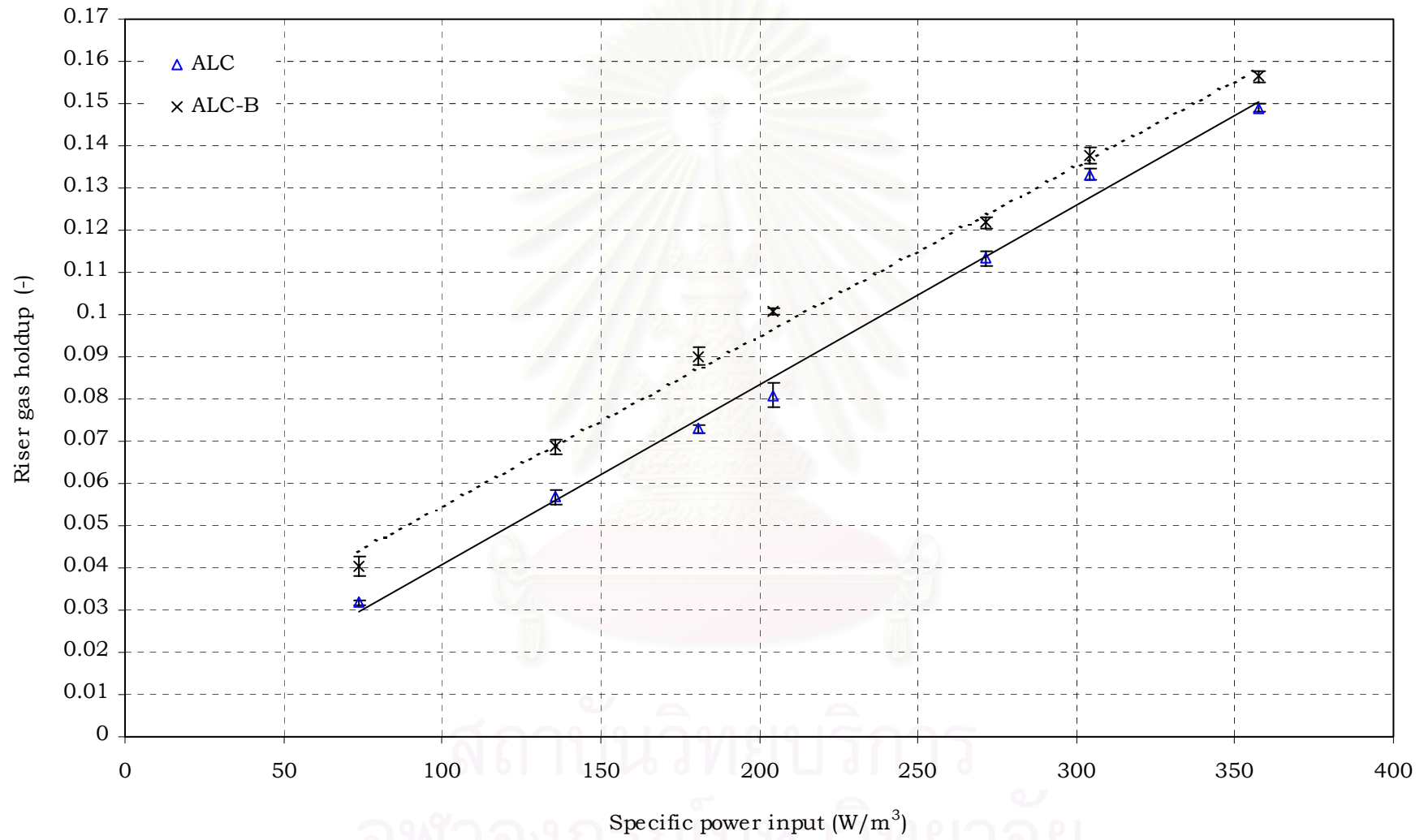


Figure 4.8 Relationship between riser gas holdup and specific power input in various configurations of ALCs

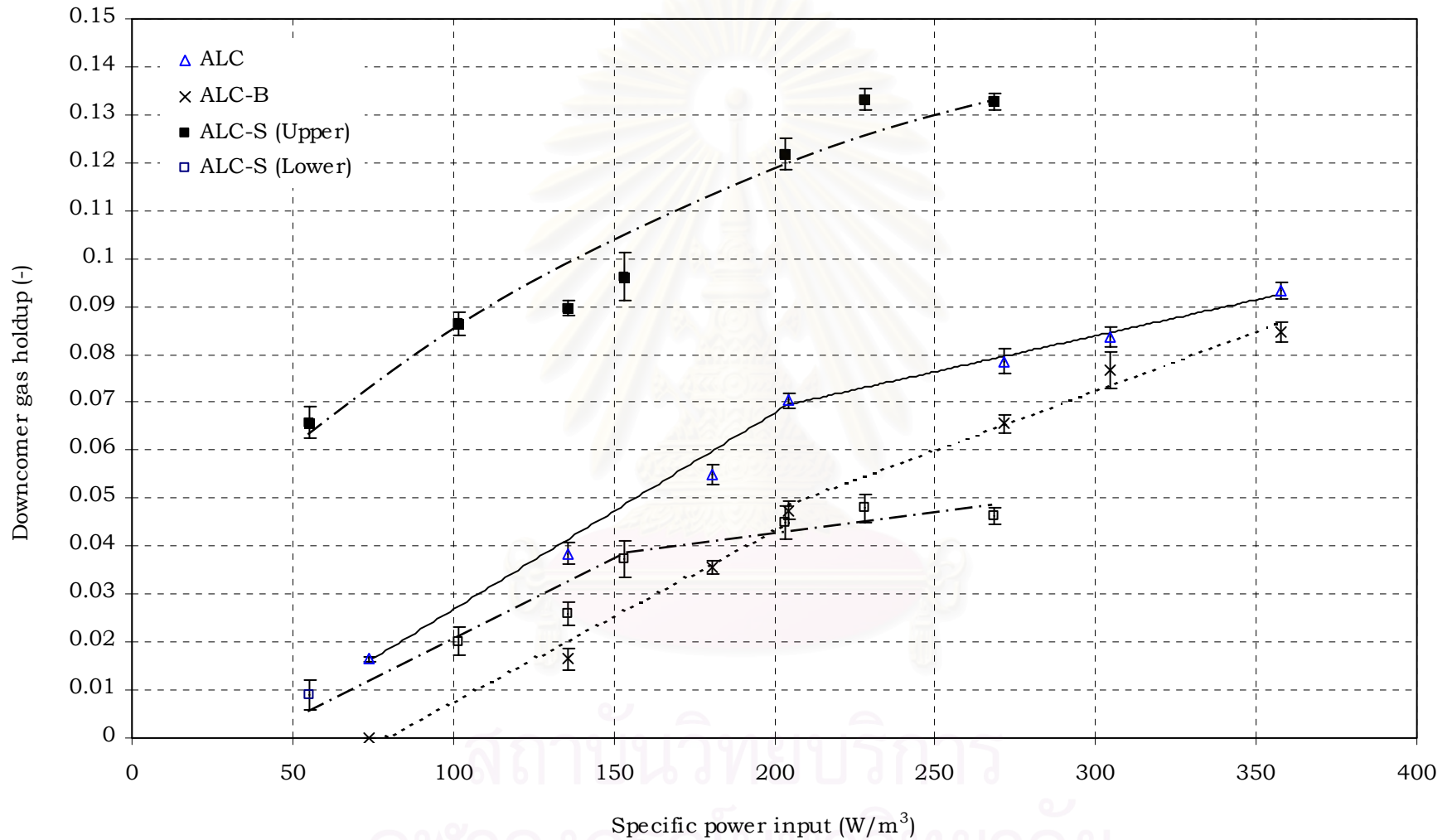


Figure 4.9 Relationship between downcomer gas holdup and specific power input in various configurations of ALCs

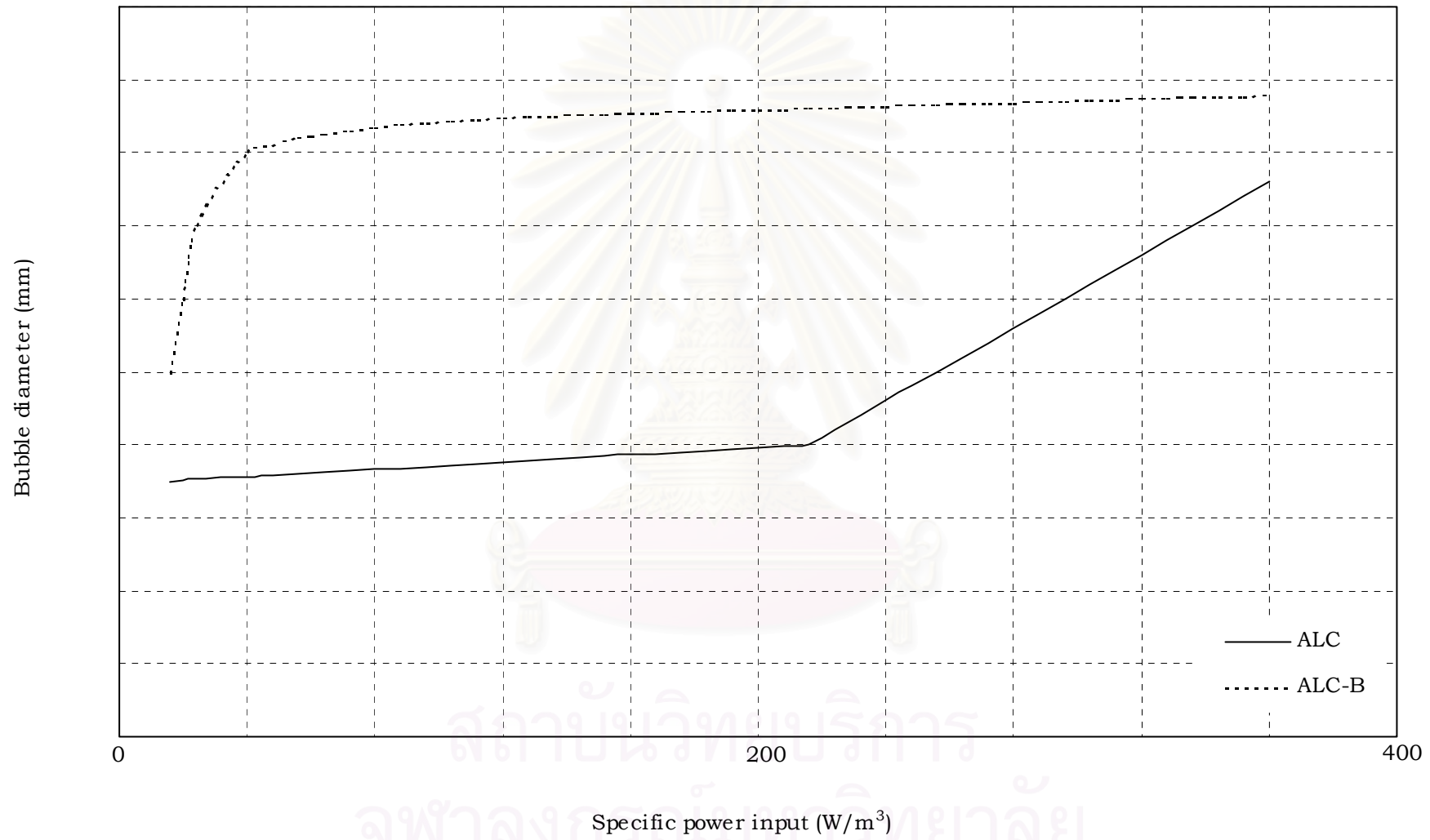


Figure 4.10 Relationship between bubble diameter and specific power input in various configurations of ALCs

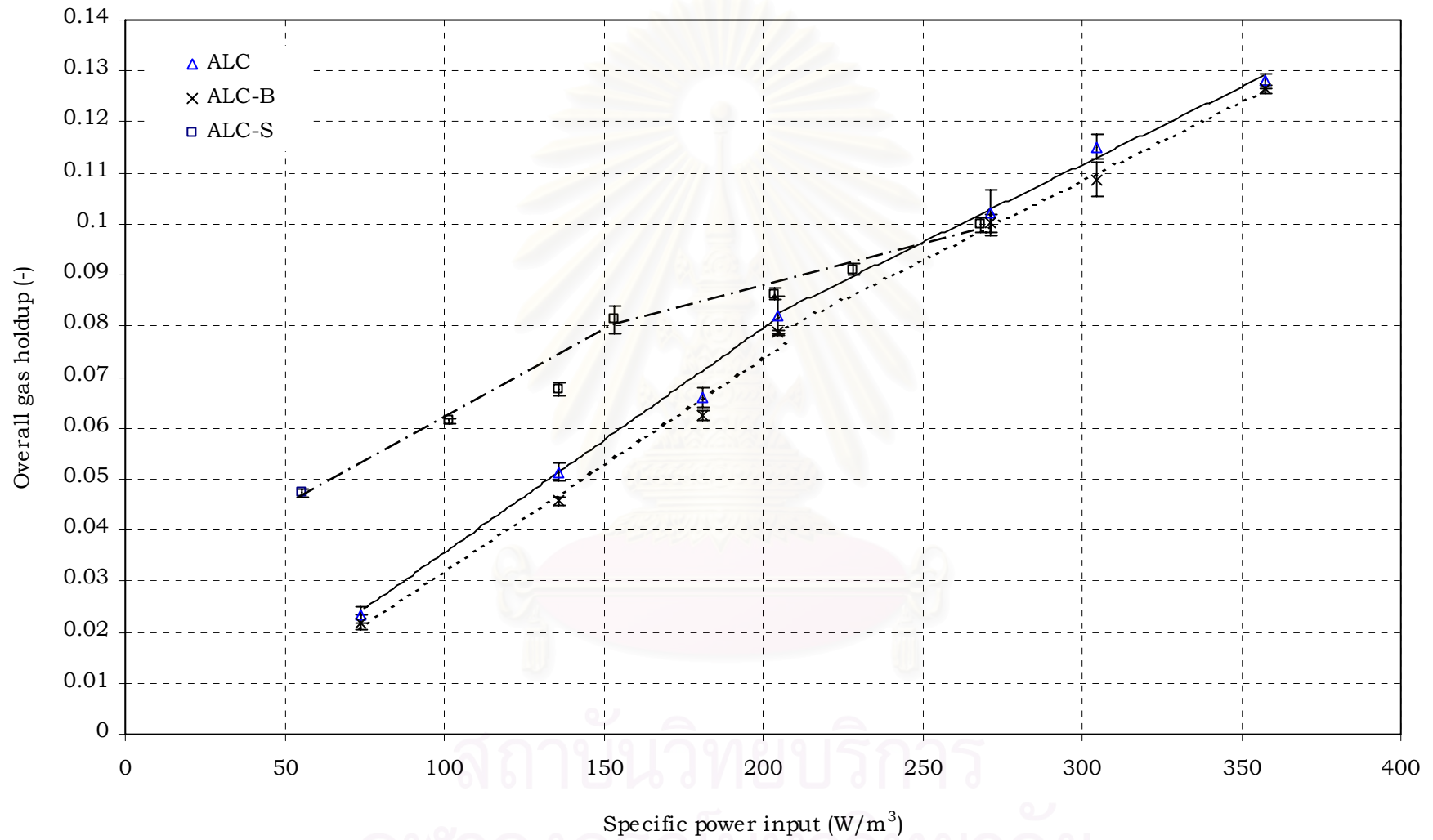


Figure 4.11 Relationship between overall gas holdup and specific power input in various configurations of ALCs

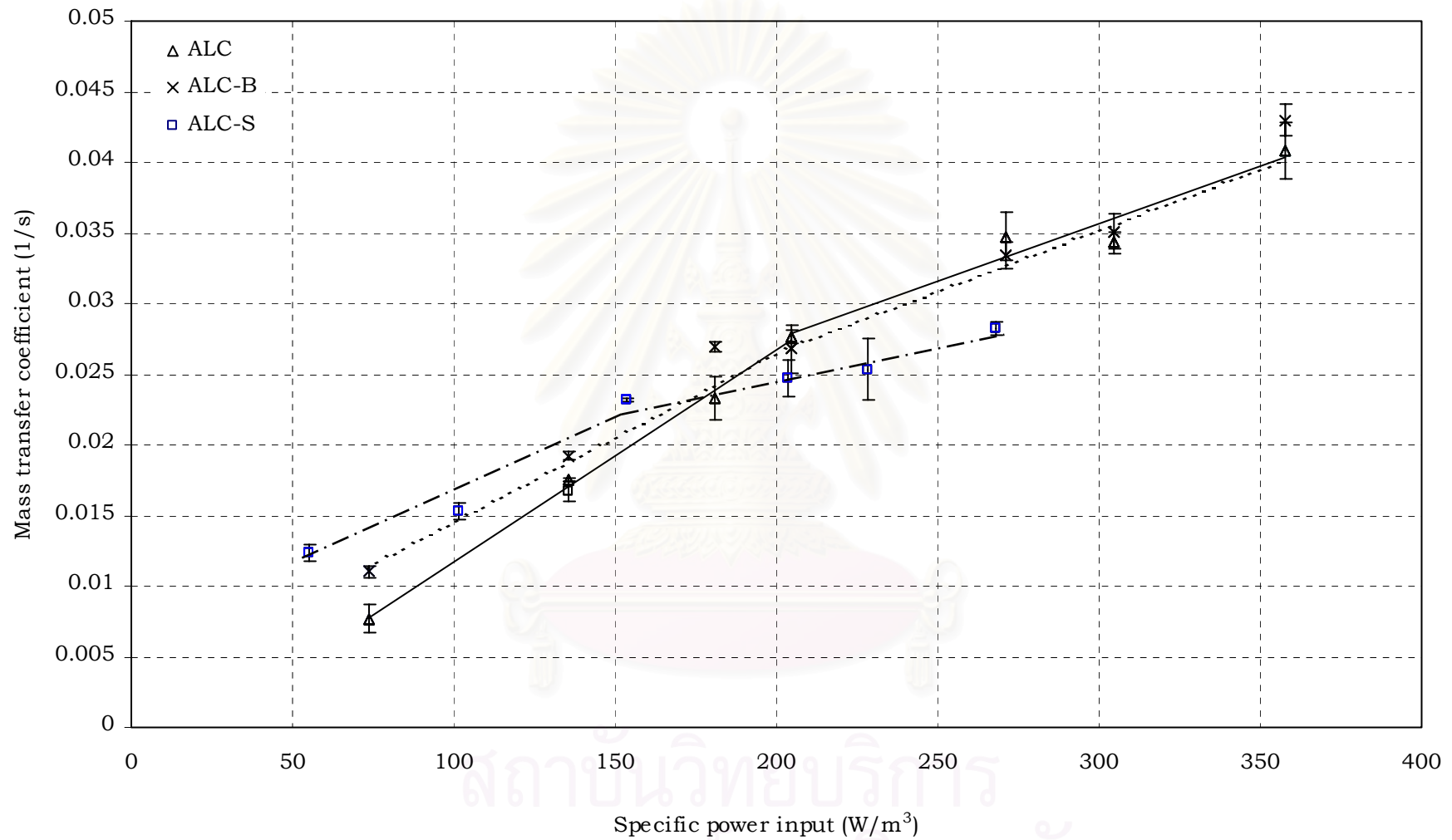


Figure 4.12 Relationship between mass transfer coefficient and specific power input in various configurations of ALCs

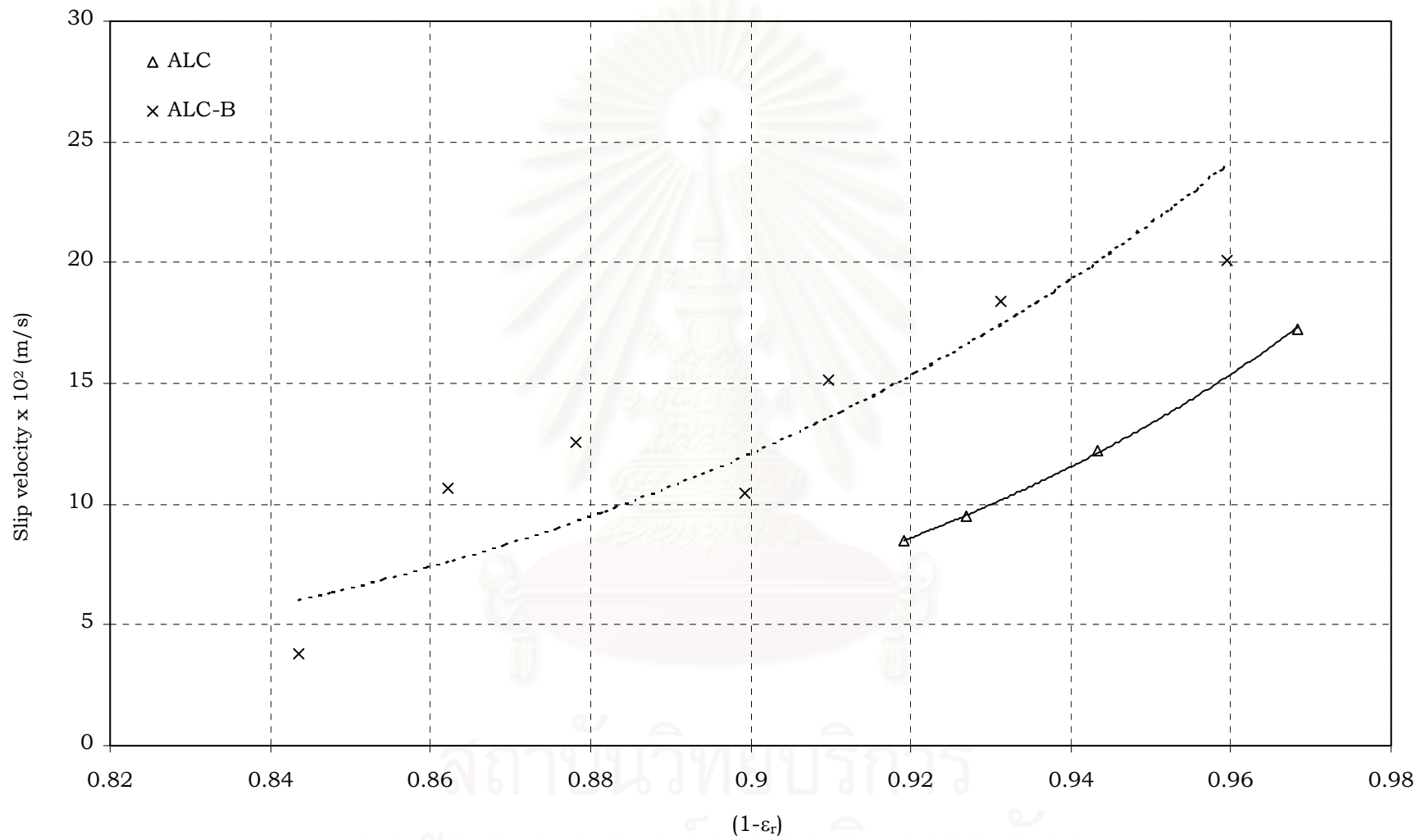


Figure 4.13 Relationship between slip velocity and riser gas holdup in various configurations of ALCs

Low P_G/V_L

Higher P_G/V_L

$P_G/V_L \approx 200 \text{ W/m}^3$

$P_G/V_L > 200 \text{ W/m}^3$

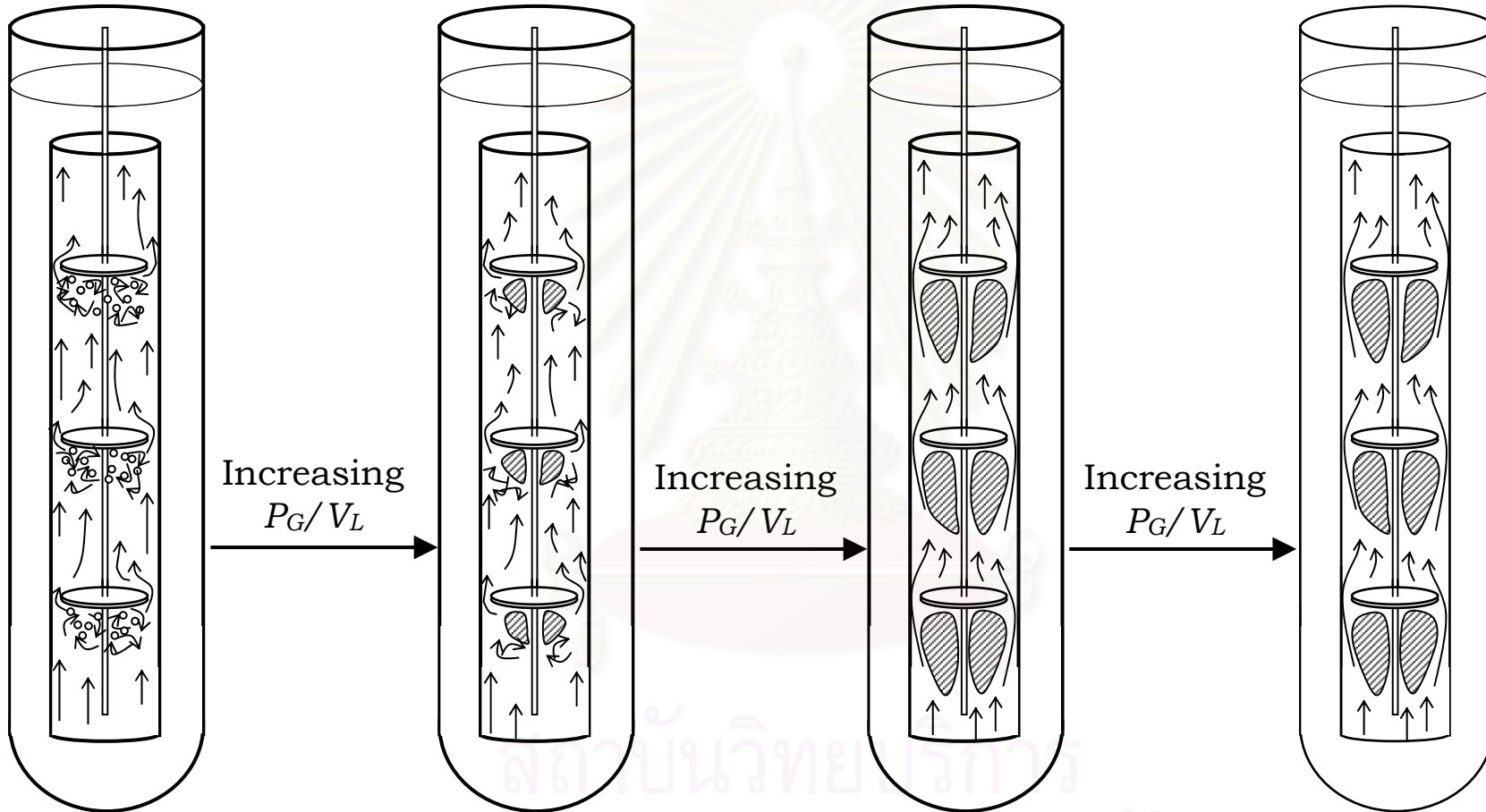


Figure 4.14 The mechanism of dead zones in the ALC-B

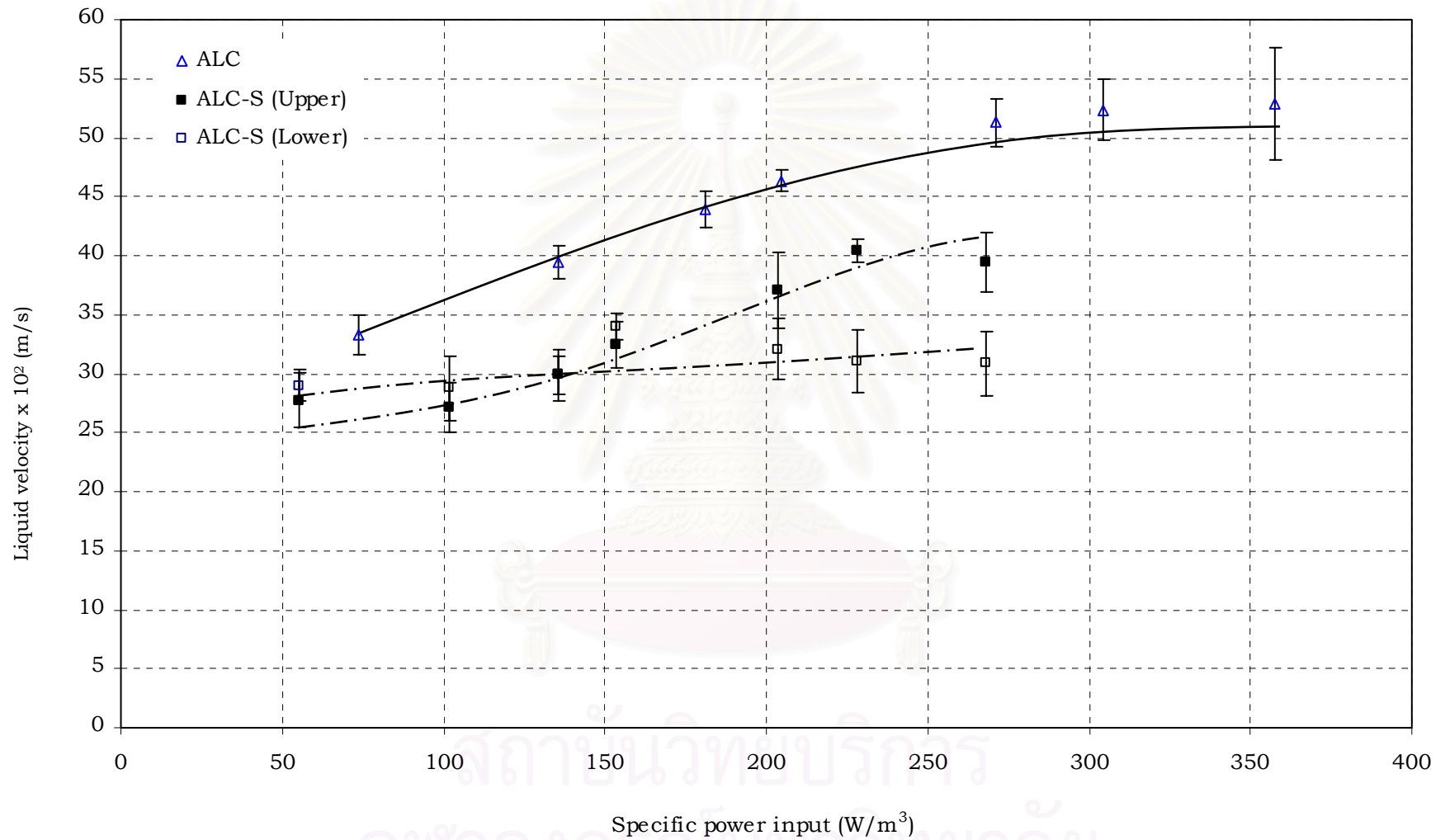


Figure 4.15 Relationship between liquid velocity and specific power input in various configurations of ALCs

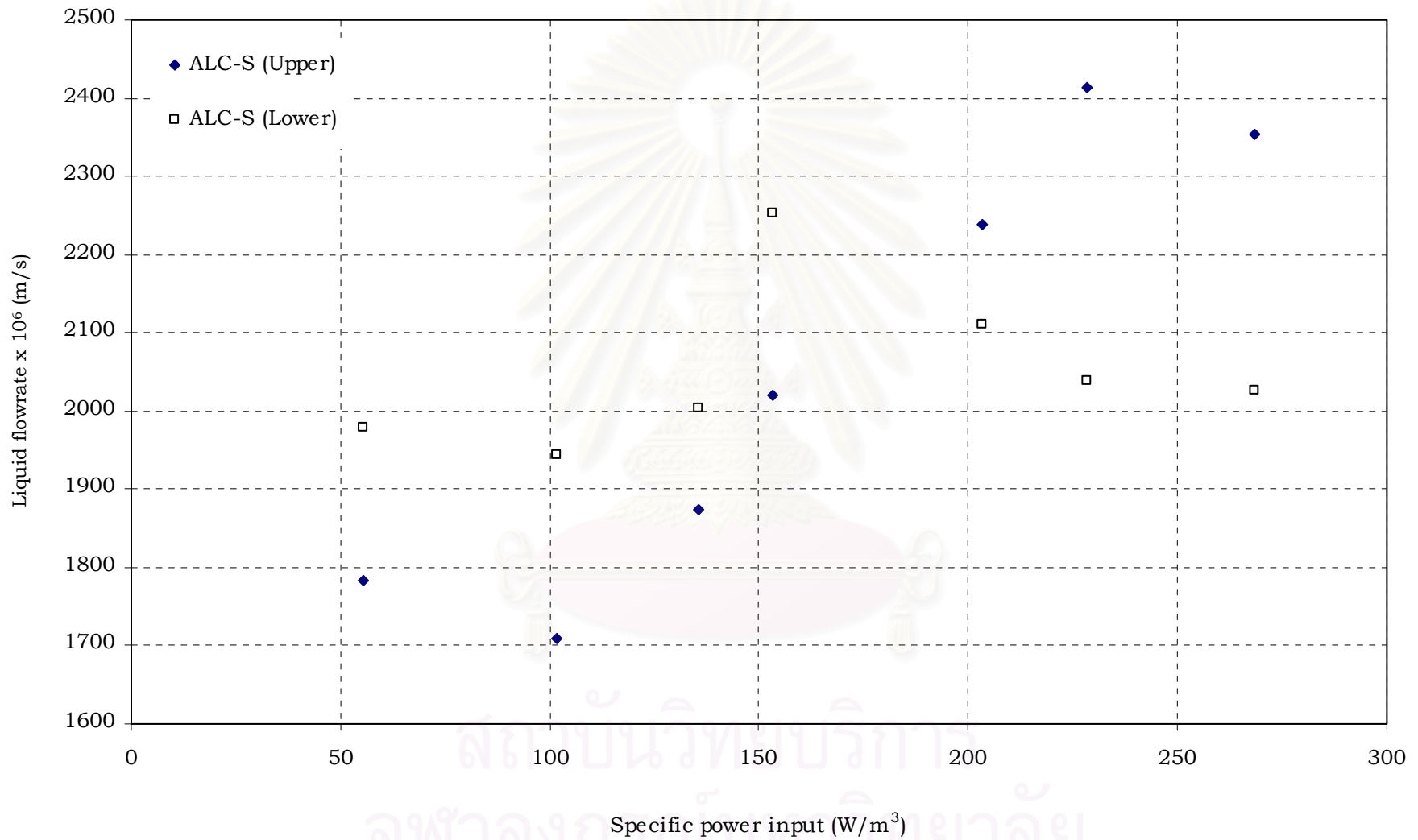


Figure 4.16 Relationship between liquid flowrate and specific power input at the upper and lower parts of ALCs

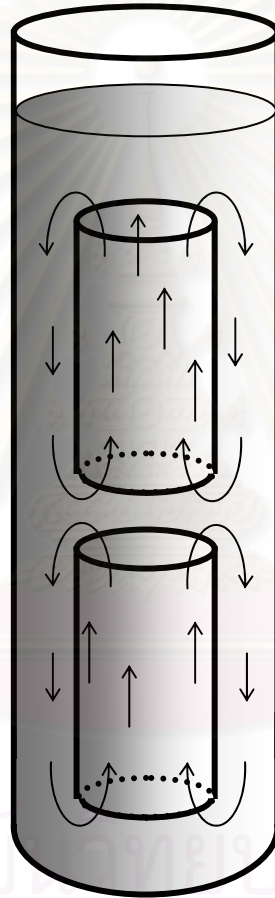


Figure 4.17 The flow path of liquid in the ALC-S

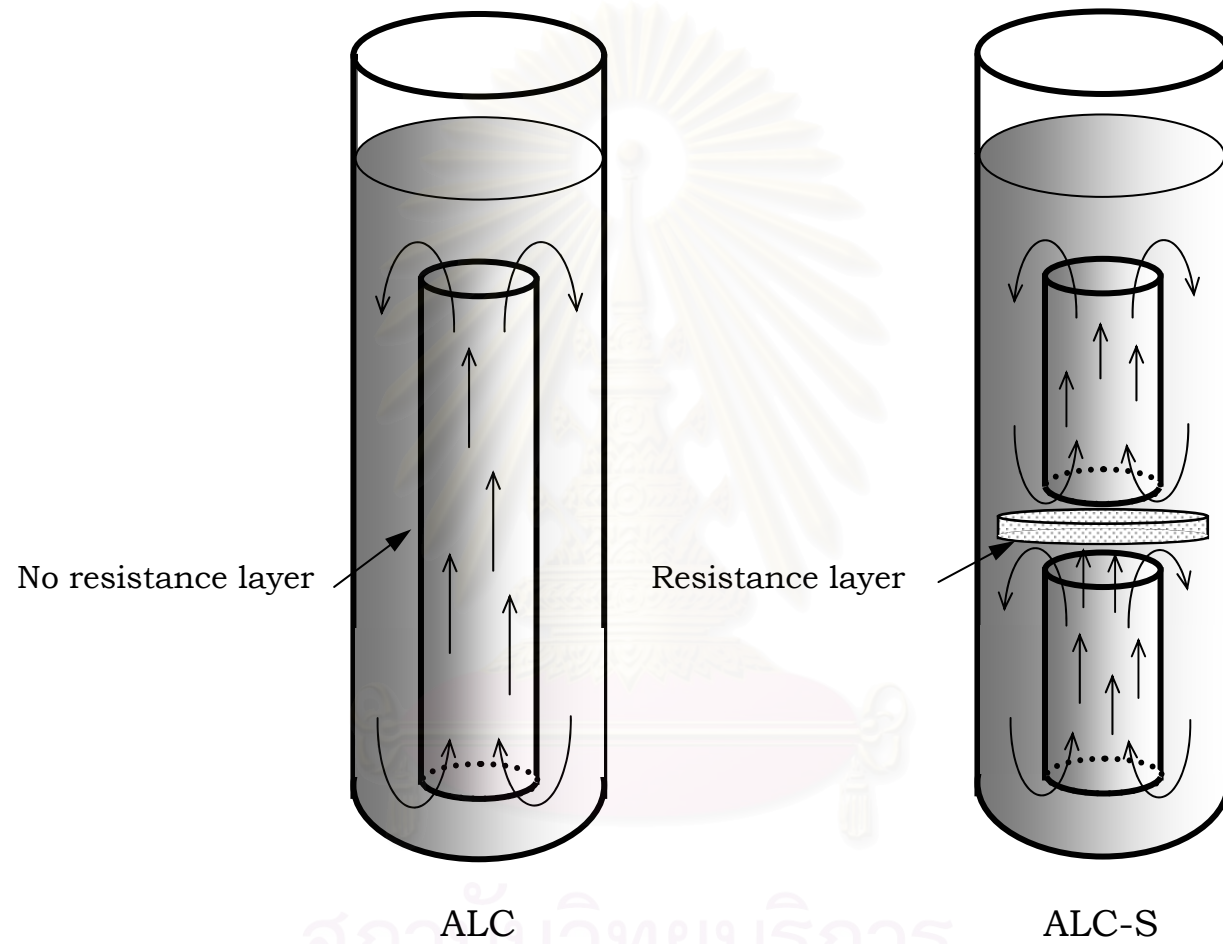


Figure 4.18 The resistance layer in the ALC-S

CHAPTER 5

CONCLUSIONS AND RECOMMENDATIONS

5.1 Effect of Specific Power Input on Hydrodynamic Behavior and Mass Transfer Performance in Airlift Contactors

The effect of P_G/V_L on hydrodynamic behavior and mass transfer performance in the conventional ALC can be summarized as following.

- i) The liquid velocity increased with increasing P_G/V_L which was due to an increase in the energy or momentum transfer from gas to liquid. However, at high P_G/V_L the liquid velocity became approximately constant because there existed a limitation on the rate of gas-liquid momentum transfer (Section 4.1.1).
- ii) The riser gas holdup linearly depended on P_G/V_L . This was attributed to an increase in the quantity of gas per unit volume that entered in the riser (Section 4.1.2).
- iii) The downcomer gas holdup had a tendency to increase steadily with enhancing P_G/V_L , which was caused by an increase in the liquid velocity. Nevertheless, at high P_G/V_L there was more bubble coalescence, and hence the increasing rate of downcomer gas holdup tended to slow down (Section 4.1.3).
- iv) The overall gas holdup increased as P_G/V_L increased, but at high P_G/V_L the rate of increase in the overall gas holdup slightly decreased. This was due to the influence of riser and downcomer gas holdups (Section 4.1.4).

- v) The increase in P_G/V_L gave rise to the mass transfer coefficient. This might be attributed to an increase in “ α ” as more gas was supplied to the system. However, at $P_G/V_L > 250 \text{ W/m}^3$ the effect of P_G/V_L on the mass transfer coefficient was slightly weak. This was due to the coalescence of bubbles (Section 4.1.5).

Experimental results in Chapter 4 can be extracted into mathematical correlations as summarized in Table 5.1.

Table 5.1 Expressions showing the relationships between hydrodynamic and mass transfer parameters with P_G/V_L in the ALC, respectively.

| Parameter | Expression* | Range of P_G/V_L | % Error |
|---------------------------|---|-----------------------------|------------|
| Liquid velocity | $v_L = 0.086P_G/V_L^{0.3142}$ | $70 \leq P_G/V_L \leq 360$ | ± 3.1 |
| Riser gas holdup | $\varepsilon_r = 0.0004P_G/V_L^{0.9948}$ | $70 \leq P_G/V_L \leq 360$ | ± 7.5 |
| Downcomer gas holdup | $\varepsilon_d = 0.0004P_G/V_L - 0.0142$ | $70 \leq P_G/V_L \leq 200$ | ± 7.4 |
| | $\varepsilon_d = 0.0049P_G/V_L^{0.4977}$ | $200 \leq P_G/V_L \leq 360$ | ± 2.2 |
| Overall gas holdup | $\varepsilon_o = 0.000145P_G/V_L^{1.2}$ | $70 \leq P_G/V_L \leq 200$ | ± 12.5 |
| | $\varepsilon_o = 0.0011P_G/V_L^{0.8574}$ | $200 \leq P_G/V_L \leq 360$ | ± 3.3 |
| Mass transfer coefficient | $k_La = 0.000155P_G/V_L - 0.0033$ | $70 \leq P_G/V_L \leq 200$ | ± 5.8 |
| | $k_La = 8 \times 10^{-5}P_G/V_L + 0.0112$ | $200 \leq P_G/V_L \leq 360$ | ± 3.5 |

$[v_L] = \text{m/s}$; $[P_G/V_L] = \text{W/m}^3$; $[\varepsilon] = \text{dimensionless}$; $[k_La] = 1/\text{s}$

*These correlations are specific to the ALC with dimension shown in Table 3.1.

5.2 Effect of Baffles on Hydrodynamic Behavior and Mass Transfer Performance in Airlift Contactors

The influence of baffles on hydrodynamic behavior and mass transfer performance can be concluded as follows.

- i) The introduction of baffles into the ALC led to a decrease in the liquid velocity. This was because of an increase in a resistance to liquid flow (Section 4.2.1).
- ii) The baffles obstructed the rise of bubbles resulting in an increase in the residence time of bubbles. In addition, baffles also retarded the liquid velocity leading to an increase in the residence time of bubbles. Therefore a more favorable riser gas holdup was obtained in the ALC-B. At high P_G/V_L , however, the riser gas holdups in the ALC-B and the ALC did not differ significantly from each other. This was because the reduction in the increasing rate of liquid velocity in the ALC-B with P_G/V_L was not as severe as that in the ALC (Section 4.2.2).
- iii) The downcomer gas holdup, which was obtained from the ALC-B, was lower than that in the ALC. This was due to the slower liquid velocity in the ALC-B that caused fewer bubbles being moved down in to the downcomer. But at high P_G/V_L the downcomer gas holdup in the baffles system seemed closer to the downcomer gas holdup obtained in the ALC (Section 4.2.3).
- iv) The overall gas holdup in the ALC-B was slightly less than that in the ALC. This was due to the influence of the gas holdups in riser and downcomer (Section 4.2.4).
- v) Baffles exerted two opposing impact on gas-liquid mass transfer coefficient: (1) baffles facilitated the coalescence of bubbles which resulted in the reduction of the gas-liquid interfacial area

(a); and (2) baffles caused severe turbulence resulting in an increase in “ k_L ”. The overall mass transfer coefficient ($k_L a$) was found to be influenced by “ k_L ” rather than “ a ” in this case. Hence it was observed that the $k_L a$ in ALC-B was higher than that in ALC. However, at high P_G/V_L baffles seemed to create dead zones and the effect of baffles on mass transfer disappeared (Section 4.2.5).

The effect of baffles can be mathematically expressed into empirical correlations as summarized in Table 5.2.

Table 5.2 Expressions showing the relationships between hydrodynamic and mass transfer parameters with P_G/V_L in the ALC-B, respectively.

| Parameter | Expression* | Range of P_G/V_L | % Error |
|---------------------------|--|-----------------------------|------------|
| Liquid velocity | $v_L = 0.02946P_G/V_L^{0.4854}$ | $70 \leq P_G/V_L \leq 360$ | ± 7.0 |
| Riser gas holdup | $\varepsilon_r = 0.001P_G/V_L^{0.8552}$ | $70 \leq P_G/V_L \leq 360$ | ± 6.1 |
| Downcomer gas holdup | $\varepsilon_d = 0.00034P_G/V_L - 0.0287$ | $70 \leq P_G/V_L \leq 200$ | ± 14.0 |
| | $\varepsilon_d = 0.000175P_G/V_L^{1.0649}$ | $200 \leq P_G/V_L \leq 360$ | ± 7.6 |
| Overall gas holdup | $\varepsilon_o = 0.000114P_G/V_L^{1.2225}$ | $70 \leq P_G/V_L \leq 200$ | ± 4.9 |
| | $\varepsilon_o = 0.0009P_G/V_L^{0.84124}$ | $200 \leq P_G/V_L \leq 360$ | ± 1.7 |
| Mass transfer coefficient | $k_L a = 0.00013P_G/V_L + 0.0017$ | $70 \leq P_G/V_L \leq 200$ | ± 5.7 |
| | $k_L a = 0.0001/V_L + 0.0053$ | $200 \leq P_G/V_L \leq 360$ | ± 4.5 |

$[v_L] = \text{m/s}$; $[P_G/V_L] = \text{W/m}^3$; $[\varepsilon] = \text{dimensionless}$; $[k_L a] = 1/\text{s}$

*These correlations are specific to the ALC-B with dimension shown in Table 3.1.

5.3 Effect of Vertically Split Draft Tube on Hydrodynamic Behavior and Mass Transfer Performance in Airlift Contactors

The effect of vertically split draft tube on hydrodynamic behavior and mass transfer performance can be extracted as following.

- i) The liquid velocity in the ALC-S was lower than that in the ALC. This can be explained as followed. In the ALC-S there existed a resistance layer between the upper and lower parts, and this layer negatively influenced the liquid velocity. Therefore the movement of liquid in the ALC-S was slower than that in the ALC (Section 4.3.1).
- ii) The downcomer gas holdup at upper part of ALC-S was higher than that in the ALC. This might be attributed to an increase in a number of small bubbles in the riser of the ALC-S which resulted in the more chance of bubbles being migrated into the downcomer. On the other hand, the downcomer gas holdup at the lower part of the ALC-S was lower than that in the ALC. This was because the quantity of gas per unit volume supplied at this part was lower than that in the ALC (Section 4.3.2).
- iii) The overall gas holdup was greater in the ALC-S than in the ALC at low P_G/V_L . This was because of the influence of the bubble size and the liquid velocity that increased the residence time of bubble in the ALC-S. However, at high P_G/V_L the rate of increase in the overall gas holdup in ALC-S seemed to decline. This was expected to be due to the reduction of the increasing rate in riser gas holdup (Section 4.3.3).
- iv) The mass transfer coefficient obtained in the ALC-S was higher than that in the ALC at low P_G/V_L . This was explained by considering two effects. Firstly, there was a lot of small bubbles

in the ALC-S leading to a higher the specific gas-liquid interfacial area. Secondly, the ALC-S had a higher overall gas holdup which gave the positive effect on specific gas-liquid interfacial area. Nevertheless, at high P_G/V_L the increasing rate of the mass transfer coefficient in the ALC-S decreased, and the value of $k_L a$ seemed to be lower than that in the ALC. This was due to an reduction in the increasing rate of overall gas holdup (Section 4.3.4).

The effect of vertically split draft tube can be mathematically extracted into empirical correlations as summarized in Table 5.3.

Table 5.3 Expressions showing the relationships between hydrodynamic and mass transfer parameter with P_G/V_L in the ALC-S, respectively.

| Parameter | Expression* | Range of P_G/V_L | % Error |
|---------------------------|--|-----------------------------|------------|
| Liquid velocity | | | |
| Upper part | $v_{Lup} = 0.084102P_G/V_L^{0.2744}$ | $55 \leq P_G/V_L \leq 270$ | ± 18.8 |
| Lower part | $v_{Llw} = 0.22617P_G/V_L^{0.0617}$ | $55 \leq P_G/V_L \leq 270$ | ± 17.3 |
| Downcomer gas holdup | | | |
| Upper part | $\varepsilon_{dup} = 0.0096P_G/V_L^{0.4721}$ | $55 \leq P_G/V_L \leq 270$ | ± 8.8 |
| Lower part | $\varepsilon_{dlw} = 0.0003P_G/V_L - 0.0079$ | $55 \leq P_G/V_L \leq 155$ | ± 15.9 |
| | $\varepsilon_{dlw} = 0.0046P_G/V_L^{0.4225}$ | $155 \leq P_G/V_L \leq 270$ | ± 5.2 |
| Overall gas holdup | $\varepsilon_o = 0.0004P_G/V_L - 0.0142$ | $55 \leq P_G/V_L \leq 155$ | ± 6.5 |
| | $\varepsilon_o = 0.0049P_G/V_L^{0.4977}$ | $155 \leq P_G/V_L \leq 270$ | ± 2.3 |
| Mass transfer coefficient | $k_L a = 0.0001P_G/V_L + 0.005$ | $55 \leq P_G/V_L \leq 155$ | ± 12.1 |
| | $k_L a = 4E-05P_G/V_L + 0.0162$ | $155 \leq P_G/V_L \leq 270$ | ± 4.5 |

$[v_L] = \text{m/s}$; $[P_G/V_L] = \text{W/m}^3$; $[\varepsilon] = \text{dimensionless}$; $[k_L a] = 1/\text{s}$

*These correlations are specific to the ALC-S with dimension shown in Table 3.1.

5.4 Concluding Remarks

Statistics were employed to improve the reliability of experimental results obtained from this work. However, theory about Airlift Contactors is still not fully understood. One reason for this is that the measurement are still not available for several operating parameters such as “gas bubble diameter”, “bubble size distribution”, “bubble velocity” and “variation in velocities”, etc. Once these techniques are developed, we will be able to understand more thoroughly the various facts of transport mechanisms in the ALC.



สถาบันวิทยบริการ
จุฬาลงกรณ์มหาวิทยาลัย

REFERENCES

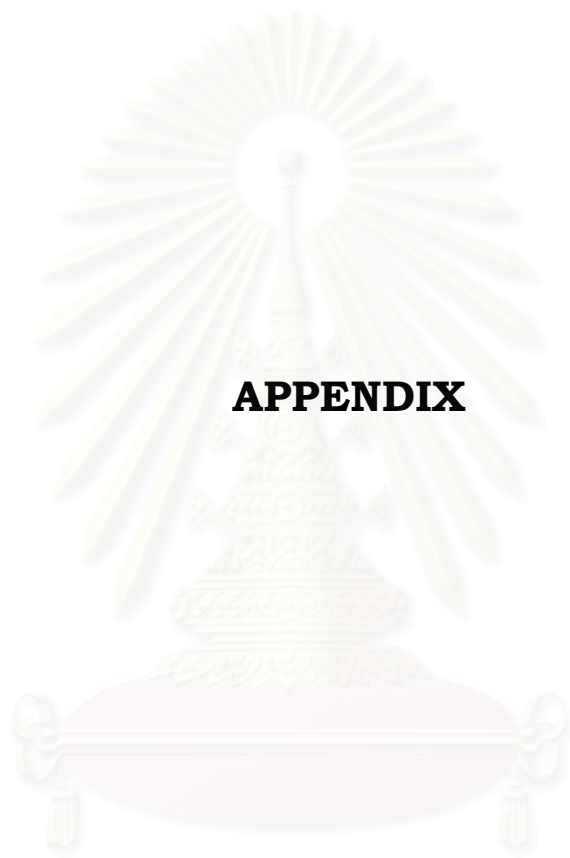
- Akita, K. Okazaki, T. and Koyama, H. 1988. Gas holdups and friction factors of gas-liquid two-phase flow in an air-lift bubble column. *J. Chem. Eng. Japan* 21: 476-482.
- Akita, K., Nakanishi, O. and Tsuchiya, K. 1994. Turn-around energy losses in an external-loop airlift reactors. *Chem. Eng. Sci.* 15: 2521-2533.
- Al-Masry, W.A. and Abasaed, A.E. 1998. On the scale up of external loop airlift reactors: Newtonian systems. *Chem. Eng. Sci.* 53: 4085-4094.
- Bando, Y., Nishimura, M., Sota, H. and Suzuki, S. 1992. Flow characteristics of countercurrent bubble column with perforated draft tube. *Chem. Eng. Sci.* 47: 3371-3378.
- Bang, W., Nikov, I., Delmas, H. and Bascoul, A. 1998. Gas-liquid mass transfer in a new tree phase stirred airlift reactor. *J. Chem. Technol. Biotechnol.* 72: 137-142.
- Bello, R.A., Robinson, C.W. and Moo-Young, M. 1985. Gas hold up and overall volumetric oxygen transfer coefficient in airlift contactors. *Biotech. Bioeng.* 27: 369-381.
- Bentifraouine, B., Xuereb, C. and Riba J.-P. 1997a. An experimental study of the hydrodynamic characteristics of external loop airlift contactors. *J. Chem. Tech. Biotechnol.* 69: 345-349.
- Bentifraouine, B., Xuereb, C. and Riba, J.-P. 1997b. Effect of gas liquid separator and liquid height on the global hydrodynamic parameters of an external-loop airlift contactor. *Chem. Eng. J.* 66: 91-95.
- Benyahia, F., Jones, L., Petit, S. and Plantaz, D. 1996. Mass transfer studies in pneumatic reactors. *Chem. Eng. Technol.* 19: 425-431.
- Calvo, E.G. 1991. A fluid dynamic model for bubble columns and airlift reactors. *Chem. Eng. Sci.* 46: 2947-2951.
- Calvo, E.G. 1992. Fluid dynamics of airlift reactors: two-phase friction factors. *AIChE. J.* 38: 1662-1666.
- Chen, C.-P., Yang, S.-J. and Wu, W.T. 1997. A novel rectangular airlift reactor with mesh baffle-plates. *Biotech. Tech.* 11: 439-441.
- Chisti, M.Y. and Moo-Young, M. 1987. Airlift reactors: characteristics, applications and design considerations. *Chem. Eng. Comm.* 60: 195-242.

- Chisti, M.Y. and Moo-Young, M. 1988. Hydrodynamics and oxygen transfer in pneumatic bioreactor devices. *Biotech. Bioeng.* 31: 487-494.
- Chisti, M.Y. 1989. *Airlift bioreactors*. New York: Elsevier Science.
- Choi, K.H. and Lee, W.K. 1990. Recirculation and flow structures of gas in downcomer section of a concentric cylindrical airlift reactor. *J. Chem. Tech. Biotech.* 48: 81-95.
- Choi, K.H. and Lee, W.K. 1993. Circulation liquid velocity, gas holdup and volumetric oxygen transfer coefficient in external-loop airlift reactors. *J. Chem. Tech. Biotechnol.* 56: 51-58.
- Choi, K.H., Chisti, Y. and Moo-young, M. 1995. Influence of the gas-liquid separator design on hydrodynamic and mass transfer performance of split-channel airlift reactors. *J. Chem. Tech. Biotechnol.* 62: 327-332.
- Clark, N.N. and Flemmer, R.L. 1985. Prediction in the holdup in two-phase bubble upflow and downflow using the Zuber and Findlay drift-flux model. *AIChE, J.* 31: 500-503.
- Couvert, A., Roustan, M. and Chatellier, P. 1999. Two-phase hydrodynamic study of a rectangular air-lift loop reactor with an internal baffle. *Chem. Eng. Sci.* 54: 5245-5252.
- Davidson, J.F. and Harrison, D. 1966. The behaviour of a continuously bubbling fluidised bed. *Chem. Eng. Sci.* 21: 731-738.
- Dussap, G. and Gros, J.B. 1982. Energy consumption and interfacial mass transfer area in an air-lift fermentor. *Chem. Eng. J.* 25: 151-162.
- Freitas, C. and Teixeira, J.A. 1998. Hydrodynamic studies in an airlift reactor with an enlarged degassing zone. *Bioproc. Eng.* 18: 267-279.
- Gavrilescu, M. and Tudose, R.Z. 1995. Study of the liquid circulation velocity in external-loop airlift bioreactors. 14: 33-39.
- Gavrilescu, M., Roman, R.V. and Tudose, R.Z. 1997. Hydrodynamics in external-loop airlift bioreactors with static mixers. *Bioproc. Bioeng.* 16: 93-99.
- Gavrilescu, M. and Tudose, R.Z. 1998. Hydrodynamics of non-Newtonian liquids in external-loop airlift reactors. *Bioproc. Bioeng.* 18: 83-89.
- Godo, S., Klein, J., Polakovic, M. and Bales, V. 1999. Periodical changes of input air flowrate - a possible way of improvement of oxygen transfer and liquid circulation in airlift bioreactors. *Chem. Eng. Sci.* 54: 4937-4943.

- Guo, Y.X., Rathor, M.N. and Ti, H.C. 1997. Hydrodynamics and mass transfer studies in a novel external-loop airlift reactor. *Chem. Eng. J.* 67: 205-214.
- Hsiun, D.-Y. and Wu, W.-T. 1995. Mass transfer and liquid mixing in an airlift reactor with a net draft tube. *Bioproc. Eng.* 12: 221-225.
- Jones, A.G. 1985. Liquid circulation in a draft-tube bubble column. *Chem. Eng. Sci.* 40: 449-462.
- Joshi, J.B. and Lali, A.M. 1984. Frontiers in Chemical Reaction Engineering. New York: Elsevier Science.
- Karamanev, D.G., Chavarie, C. and Samson, R. 1996. Hydrodynamics and mass transfer in an airlift reactor with a semipermeable draft tube. *Chem. Eng. Sci.* 51: 1173-1176.
- Kawalec-Pietrenko, B. and Holowacz, I. 1998. Region-dependent oxygen transfer rate in rectangular airlift reactor. *Bioproc. Eng.* 18: 163-170.
- Kawase, Y., Omori, N. and Tsujimura, M. 1994. Liquid-phase mixing in external-loop airlift bioreactors. *J. Chem. Tech. Biotechnol.* 61: 49-55.
- Kawase, Y., Tsujimura, M. and Yamaguchi, T. 1995. Gas hold-up in external-loop airlift bioreactors. *Bioproc. Eng.* 12: 21-27.
- Kemblowski, Z., Przywarski, J. and Diab, A. 1993. An average gas hold-up and liquid circulation velocity in airlift reactors with external loop. 48: 4023-4035.
- Koide, K., Sato, H. and Iwamoto, S. 1983. Gas holdup and volumetric liquid-phase mass transfer coefficient in bubble column with draught tube and with gas dispersion into annulus. *J. Chem. Eng. Japan.* 16: 407-419.
- Koide, K., Iwamoto, S., Takasaka, Y., Kimura, M. and Kubota, H. 1984. Liquid circulation, gas holdup and pressure drop in bubble column with draught tube. *J. Chem. Eng. Japan.* 17: 611-618.
- Korpijarvi, J., Oinas, P. and Reunanen, J. 1999. Hydrodynamics and mass transfer in an airlift reactor. *Chem. Eng. Sci.* 54: 2255-2262.
- Lin, C.H., Fang, B.S., Wu, C.S., Fang, H.Y., Kuo, T.F. and Hu, C.Y. 1976. Oxygen transfer and mixing in a tower cycling fermentor. *Biotechnol. Bioeng.* 18: 1557-1572.
- Lockett, M. and Kirkpatrick, R.D. 1975. Ideal bubbly flow and actual flow in bubble columns. *Trans. Instn. Chem. Engrs.* 53: 267-273.

- Lu, W.J. and Hwang S.J. 1994. Liquid mixing in internal loop airlift reactors. *Ind. Eng. Chem. Res.* 33: 2180-2186.
- Margaritis, A. and Sheppard, J.D. 1981. Mixing time and oxygen transfer characteristics of a double draft tube airlift fermentor. *Biotech. Bioeng.* 23: 2117-2135.
- Marrucci, G. 1965. Rising velocity of a swarm of spherical bubbles. *Ind. Eng. Chem. Fundam.* 4: 224-225.
- Merchuk, J.C. and Stein, Y. 1981. Local hold up and liquid velocity in airlift reactors. *AIChE J.* 27: 377-388.
- Merchuk, J.C. and Siegel, M. 1988. Air-lift reactors in chemical and biological technology. *J. Chem. Tech. Biotechnol.* 41: 105-120.
- Merchuk, J.C., Ladwa, N., Cameron, A., Bulmer, M. and Pickett, A. 1994. Concentric-tube airlift reactors: effects of geometrical design on performance. *AIChE J.* 40: 1105-1117.
- Merchuk, J.C. and Berzin, I. 1995. Distribution of energy dissipation in airlift reactors. *Chem. Eng. Sci.* 50: 2225-2233.
- Merchuk, J.C., Ladwa, N., Cameron, A., Bulmer, M. and Pickett, A. 1996. Liquid flow and mixing in concentric tube air-lift reactors. *J. Chem. Tech. Biotechnol.* 66: 174-182.
- Merchuk, J.C., Contreras, A., Garcia, F., and Molina, E. 1998. Studies of mixing in a concentric tube airlift bioreactor with different spargers. *Chem. Eng. Sci.* 53: 709-719.
- Onken, U. and Weiland, P. 1980. Hydrodynamics and mass transfer in an airlift loop fermentor. *European J. Appl. Microbiol Biotechnol* 10: 31-40.
- Orazem, M.E., and Erickson, L.E. 1979. Oxygen-transfer rates and efficiencies in one-and two-stage airlift towers. *Biotech. Bioeng.* 21: 69-88.
- Popovic, M.K. and Robinson, C.W. 1989. Mass transfer studies of external-loop airlifts and a bubble column. *AIChE J.* 35: 393-402.
- Prince, M.J. and Blanch, H.W. 1990. Bubble coalescence and break-up in air-sparged bubble columns. *AIChE J.* 36: 1485-1499.
- Richardson, J.F. and Zaki, W.N. 1954. Sedimentation and fluidisation: part I. *Trans. Instn. Chem. Engrs.* 32: 35-53.

- Russell, A.B., Thomas, C.R. and Lilly, M.D. 1994. The influence of vessel height and top-section size on the hydrodynamic characteristics of airlift fermentors. *Biotechnol. Bioeng.* 43: 69-76.
- Siegel, M.H., Merchuk, J.C. and Schugerl, K. 1986. Air-lift reactor analysis: interrelationships between riser, downcomer, and gas-liquid separator behavior, including gas recirculation effects. *AIChE J.* 32: 1585-1596.
- Snape, J.B., Zahradnid, J., Fialova, M. and Thomas, N.H. 1995. Liquid-phase properties and sparger design effects in an external-loop airlift reactor. *Chem. Eng. Sci.* 50: 3175-3186.
- Stejskal, J. and Potucek, F. 1985. Oxygen transfer in liquids. *Biotechnol. Bioeng.* 27: 503-508.
- Sukan, S.S. and Vardar-Sukan, F. 1987. Mixing performance of air-lift fermentors against working volume and draft tube dimensions. *Bioproc. Eng.* 2: 33-38.
- Tung, H.-L., Tu, C.-C., Chang, Y.-Y. and Wu, W.-T. 1998. Bubble characteristics and mass transfer in an airlift reactor with multiple net draft tubes. *Bioproc. Eng.* 18: 323-328.
- Utiger, M., Stuber, F., Duquenne, A.-M., Delmas, H. and Guy, C. 1999. Local measurements for the study of external loop airlift hydrodynamics. *Can. J. Chem. Eng.* 77: 375-382.
- Wachi, S., Jones, A.G. and Elson, T.P. 1991. Flow dynamics in a draft-tube bubble column using various liquids. *Chem. Eng. Sci.* 46: 657-663.
- Weiland, P. and Onken, U. 1981. Differences in the behaviour of bubble column and airlift loop reactors. *Ger. Chem. Eng.* 4: 174-181.
- Weiland, P. 1984. Influence of draft tube diameter on operation behavior of airlift loop reactors. *Ger. Chem. Eng.* 7: 374-385.
- Wu, W.-T. and Jong, J.-Z. 1994. Liquid-phase dispersion in an airlift reactor with a net draft tube. *Bioproc. Eng.* 11: 43-47.
- Young, M.A., Carbonell, R.G. and Ollis, D.F. 1991. Airlift bioreactor: analysis of local two-phase hydrodynamics. *AIChE. J.* 37: 403-428.
- Zhao, M., Niranjana, K. and Davidson, J.F. 1994. Mass transfer to viscous liquids in bubble columns and airlift reactors: influence of baffles. *Chem. Eng. Sci.* 49: 2359-2369.



APPENDIX

สถาบันวิทยบริการ
จุฬาลงกรณ์มหาวิทยาลัย

Determination of Various Parameters

Overall Gas Holdup

The volume fraction of a gas in dispersion (or the overall gas holdup) is given as:

$$\varepsilon_o = \frac{V_G}{V_D} = \frac{V_G}{V_G + V_L} \quad (\text{A.1})$$

where V_G and V_D are equal to $(A_r + A_d)(H_D - H_L)$ and $(A_r + A_d)H_D$, respectively.

Therefore,

$$\varepsilon_o = \frac{(H_D - H_L)}{H_D} \quad (\text{A.2})$$

Manometric Determination of the Fractional Gas Holdup

From Figure A.1 the mean gas holdup between point 1 and point 2 in the contactor is obtained as followed:

The pressure across a-a (Figure A.1) is equal in the two arms of the manometer, therefore,

$$P_{atm} + \rho_D g(h_1 + \Delta h) + \rho_G g(h_2 + \Delta z) = P_{atm} + \rho_D g h_1 + \rho_G g(\Delta h + h_2) + \rho_L g \Delta z \quad (\text{A.3})$$

The density of the dispersion can be estimated from:

$$\rho_D = (1 - \varepsilon)\rho_L + \varepsilon\rho_G \quad (\text{A.4})$$

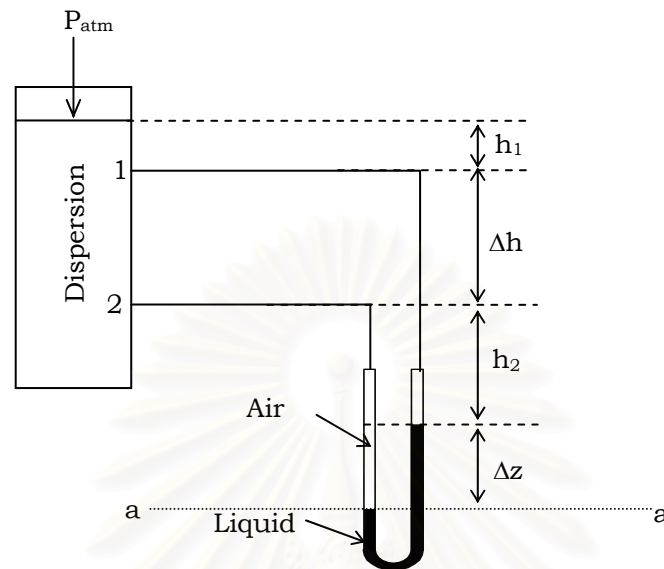


Figure A.1 The U-tube manometer setup

Substitute Equation A.4 into Equation A.3 with the assumption that ρ_G is very small and negligible, Equation A.3 becomes:

$$g(1-\varepsilon)\rho_L(h_1 + \Delta h) = g(1-\varepsilon)\rho_L h_1 + \rho_L g \Delta z \quad (\text{A.5})$$

Both sides of Equation (A.5) are divided by $\rho_L g$ to give:

$$(1-\varepsilon)(h_1 + \Delta h) = (1-\varepsilon)h_1 + \Delta z \quad (\text{A.6})$$

Hence

$$\varepsilon = 1 - \frac{\Delta z}{\Delta h} \quad (\text{A.7})$$

Riser Gas Holdups

A balance equation for the amount of gas in the reactor can be written as:

Total volume of gas = volume in the riser + volume in the downcomer +
volume in the gas-liquid separator (A.8)

Or in mathematical form as follows:

$$V_D \varepsilon_o = V_{Dr} \varepsilon_r + V_{Dd} \varepsilon_d + V_{Dgs} \varepsilon_{gs} \quad (\text{A.9})$$

Substituting V_D with $H_D(A_r + A_d)$, V_{Dr} with $H_{DT}A_r$, V_{Dd} with $H_{DT}A_d$, and V_{Dgs} with $(H_D - H_{DT})(A_d + A_r)$ yeilds:

$$H_D(A_r + A_d) \varepsilon_o = H_{DT}A_r \varepsilon_r + H_{DT}A_d \varepsilon_d + (H_D - H_{DT})(A_d + A_r) \varepsilon_{gs} \quad (\text{A.10})$$

Equation can be rearranged to:

$$\varepsilon_o = \frac{H_{DT}A_r \varepsilon_r + H_{DT}A_d \varepsilon_d}{H_D(A_r + A_d)} + \frac{(H_D - H_{DT})(A_d + A_r) \varepsilon_{gs}}{H_D(A_r + A_d)} \quad (\text{A.11})$$

It is assumed that the gas holdup in the gas-liquid separator is approximately equal to that in the riser. This allows the estimation of the riser gas holdup from the overall and downcomer gas holdups.

$$\varepsilon_o = \frac{H_{DT}A_r \varepsilon_r + H_{DT}A_d \varepsilon_d + (H_D - H_{DT})(A_d + A_r) \varepsilon_r}{H_D(A_r + A_d)} \quad (\text{A.12})$$

Therefore,

$$\varepsilon_r = \frac{\varepsilon_o H_D(A_d + A_r) - H_{DT}A_d \varepsilon_d}{H_{DT}A_r + (A_r + A_d)(H_D - H_{DT})} \quad (\text{A.13})$$

The Mass Transfer Models

The region in the vicinity of the gas-liquid interface may be visualized as consisting of adjacent, stagnant, gas and liquid films of some finite thickness as depicted in Figure A.2. The interface itself is assumed to offer

no resistance to mass transfer, therefore, the interfacial concentrations are determined by the equilibrium relationship. Mass transfer through the stagnant films is assumed to be solely by molecular diffusion and, thus at steady, linear concentration profiles exist in the films (Figure A.2). For this situation the mass flux of the diffusing species (J_{O_2}) is related to the concentration gradient (ΔC) in the film and to the film thickness (Δx) in accordance with Fick's first law:

$$J_{O_2} = \frac{D}{\Delta x} \Delta C \quad (\text{A.14})$$

where D is the molecular diffusivity of oxygen in the film. The ratio $D/\Delta x$ is known as the mass transfer coefficient, k .

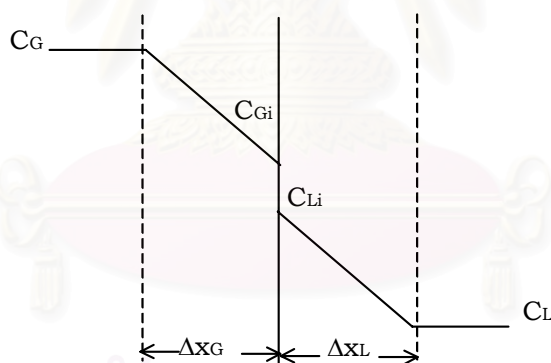


Figure A.2 The gas-liquid interface.

Equation may be written for each of the two films:

$$J_{O_2} = k_L(C_{Li} - C_L) \quad (\text{A.15})$$

where k_L is the liquid film mass transfer coefficient. Since the interfacial concentrations are in equilibrium, the flux may be expressed in terms of the overall concentration driving force as follows:

$$J_{O_2} = K_L(C^* - C_L) \quad (\text{A.16})$$

where K_L is the overall mass transfer coefficient based on liquid film. C^* saturated concentration of dissolved oxygen and C_L concentration of dissolved oxygen in liquid.

For sparingly soluble gases, it is assumed that $1/k_L \approx 1/K_L$ (Chisti, 1989). Therefore the oxygen mass flux may be expressed as:

$$J_{O_2} = k_L(C^* - C_L) \quad (\text{A.17})$$

Since the transfer rate and the flux are related by:

$$a_L J_{O_2} = \frac{dC_L}{dt} \quad (\text{A.18})$$

In terms of the rate of oxygen mass transfer, Equation A.18 may be written as:

$$\frac{dC_L}{dt} = k_L a_L (C^* - C_L) \quad (\text{A.19})$$

Specific Power Input

The work, \hat{w} , done during isothermal expansion of n moles of a gas from an initial volume, V_b , is

$$\hat{w} = \int_{V_b}^{V_t} P dV \quad (\text{A.20})$$

Assuming ideal gas behavior,

$$P = \frac{nRT}{V} \quad (\text{A.21})$$

Substitution of Equation (A.21) in Equation (A.20) followed by integration for constant T yields:

$$\hat{w} = nRT \ln \frac{V_t}{V_b} \quad (\text{A.22})$$

When both sides of Equation (A.22) are divided by the time (t) over which the work is done, Equation A.22 can be written as:

$$\frac{\hat{w}}{t} = \frac{n}{t} RT \ln \frac{V_t}{V_b} \quad (\text{A.23})$$

where n/t corresponds to molal gas flowrate (Q_m) and \hat{w}/t corresponds to the power input (P_G). Thus,

$$P_G = Q_m RT \ln \frac{V_t}{V_b} \quad (\text{A.24})$$

V_b and V_t in Equation (A.24) can be replaced by the corresponding pressures, P_b and P_t , so that

$$P_G = Q_m RT \ln \frac{P_b}{P_t} \quad (\text{A.25})$$

where the subscripts b and t denote the bottom and the top (or the head-space) of the reactor.

The substitution of

$$P_b = P_t + \rho_L g H_L \quad (\text{A.26})$$

into Equation (A.25) leads to:

$$P_G = Q_m RT \ln \frac{P_t + \rho_L g H_L}{P_t} = Q_m RT \ln \left(1 + \frac{\rho_L g H_L}{P_t} \right) \quad (\text{A.27})$$

Or, in term of the specific power input P_G/V_L ;

$$\frac{P_G}{V_L} = \frac{Q_m RT}{V_L} \ln \left(1 + \frac{\rho_L g H_L}{P_t} \right) \quad (\text{A.28})$$

Also, the mean superficial gas velocity in a reactor is:

$$U_{sg} = \frac{1}{H_L} \int_0^{H_L} \dot{U}_{sg} dl \quad (\text{A.29})$$

and the local value of the superficial gas velocity (\dot{U}_{sg}) is:

$$\dot{U}_{sg} = \frac{\bar{V}}{A} = \frac{Q_m RT}{PA} \quad (\text{A.30})$$

where \bar{V} is the local volume flowrate and A the reactor cross-sectional area. From the equations (A.29) and (A.30), for constant A , Q_m and T ,

$$U_{sg} = \frac{Q_m RT}{h_L A} \int_0^{H_L} \frac{1}{P} dl \quad (\text{A.31})$$

The substitution of

$$P = P_h + \rho_L g l \quad (\text{A.32})$$

into Equation (A.31), followed by integration, yields:

$$U_{sg} = \frac{Q_m RT}{H_L A \rho_L g} \ln \left(1 + \frac{\rho_L g H_L}{P_h} \right) \quad (\text{A.33})$$

But,

$$V_L = H_L A \quad (\text{A.34})$$

Therefore,

$$U_{sg} = \frac{Q_m RT}{V_L \rho_L g} \ln \left(1 + \frac{\rho_L g H_L}{P_h} \right) \quad (\text{A.35})$$

Comparison of Equation (A. 28) and (A. 35), yields

$$\frac{P_G}{V_L} = \rho_L g U_{sg} \quad (\text{A.36})$$

Equation (A.36) is applicable to bubble column having a constant cross-section. For airlifts for which the superficial gas velocity, U_{sgr} , is usually based on the riser cross-section. Equation (A.36) modifies to

$$\frac{P_G}{V_L} = \frac{\rho_L g U_{sgr}}{1 + \frac{A_d}{A_r}} \quad (\text{A.37})$$

Specific Gas-liquid Interfacial Area and k_L/d_B

Assuming spherical bubbles, the gas volume in dispersion is given by

$$V_G = \frac{N\pi d_B^3}{6} \quad (\text{A.38})$$

The total gas-liquid interfacial area in dispersion is given as:

$$A_L = N\pi d_B^2 \quad (\text{A.39})$$

and the specific gas-liquid interfacial area per unit unaerated liquid volume is

$$a_L = \frac{A_L}{V_L} = \frac{N\pi d_B^2}{V_L} \quad (\text{A.40})$$

From Equation A.1 we get

$$V_L = \frac{V_G(1-\varepsilon)}{\varepsilon} \quad (\text{A.41})$$

Substituting of Equation A.31 in Equation A.40 results in

$$a_L = \frac{6\varepsilon}{d_B(1-\varepsilon)} \quad (\text{A.42})$$

The both sides of Equation A.42 are multiplied with the mass transfer coefficient, k_L . Therefore,

$$k_L a = \frac{6k_L\varepsilon}{d_B(1-\varepsilon)} \quad (\text{A.43})$$

$$\frac{k_L}{d_B} = k_L a \frac{(1-\varepsilon)}{6\varepsilon} \quad (\text{A.44})$$

สถาบันวิทยบริการ
จุฬาลงกรณ์มหาวิทยาลัย

VITA

Miss Thanathorn Vorapongsathorn was born in Bangkok on December 12, 1977. She graduated high school from Traim Udom Suksa in 1993 and received her Bachelor degree in Chemical Engineering from the Department of Chemical Engineering, Faculty of Engineering, Chulalongkorn University in 1997.



สถาบันวิทยบริการ
จุฬาลงกรณ์มหาวิทยาลัย